NASA Contractor Report 158962

A RECOMMENDED ENTRY RECONSTRUCTION PROCESS FOR THE PIONEER VENUS MULTI-PROBE MISSION

J. T. Findlay
G. M. Kelly

ANALYTICAL MECHANICS ASSOCIATES, INC.
17 Research Road, Hampton, Virginia 23666

CONTRACT NAS1-15055
November, 1978

National
Aeronautics and
Space
Administration

FINAL REPORT

A RECOMMENDED ENTRY RECONSTRUCTION PROCESS FOR THE PIONEER VENUS MULTI-PROBE MISSION

by

J. T. Findlay

G. M. Kelly

AMA Report 78-18

Contract No. NAS1-15055

August, 1978

ANALYTICAL MECHANICS ASSOCIATES, INC.
17 RESEARCH ROAD
HAMPTON, VIRGINIA 23666

ABSTRACT

A method for determining the entry trajectories for the Pioneer Venus multi-probe mission is presented herein. The recommended method utilizes Earth based Doppler and on-board accelerometry as observables to provide updates for the spacecraft state and atmospheric parameters. The evolution of this method, based on error analyses and actual simulation results, is discussed in this report. A derivative of the Viking Radio Science Orbit Determination software, used by experimenters at LaRC, is recommended for the reconstruction.

The reconstruction process utilized for the Viking landers, after considerable analysis, was deemed inappropriate for the P/V mission due principally to insufficient spacecraft data. If atmospheric wind information were available one could make use of the Viking concept to obtain a first order density update to be used as a priori information in the recommended process.

Telemetry data pre-processing requirements have been defined. A cubic spline derivative routine is recommended to extract accelerations from the accumulated velocity decrements.

Recommendations are made herein for further development of the entry reconstruction and pre-processing software.

TABLE OF CONTENTS

TABLE OF CONTENTS (CON'T)

LIST OF FIGURES

LIST OF FIGURES (CON'T)

LIST OF TABLES

LIST OF SYMBOLS

Symbol	Description
A	Aerodynamic Reference area
A_x	Axial acceleration
C_D	Drag coefficient
C_L	Lift coefficient
h	Spacecraft altitude above planet surface
LAS	Large probe - Atmospheric Structures Experiment
P/V	Pioneer Venus
R	Spacecraft radius from center of planet
R_{φ}	Venus planet radius
SAS	Small probe - Atmospheric Structures Experiment
S/C	Spacecraft
V	Spacecraft velocity vector
W	Weight of spacecraft

Greek Symbols

α	Angle-of-attack
β	Side-slip angle
γ	Flight path angle of velocity vector (pos. above the horizon)
Δ	Denotes difference
φ	Spacecraft latitude
λ	Spacecraft longitude

LIST OF SYMBOLS (CON'T)

Greek Symbols	Description
ψ	Heading of the spacecraft velocity vector (pos. c/w from North)
ρ	Atmospheric density
η	Total angle-of-attack
μ_{φ}	GM of Venus
σ	Standard deviation

Subscripts

$()_o$	Initial condition @ Entry
$()_I$	Inertial quantity
$()_R$	Planet relative quantity
$()_A$	Atmosphere relative quantity

I. INTRODUCTION

The Pioneer Venus multi-probe mission, scheduled to enter the Venusian atmosphere in December of this year, will provide interesting science for the Atmospheric Structures Experiment Team. To enhance the science return, accurate entry trajectory estimates of the probes are required. It was the primary intent under this contract to define the method most suitable to enable said accurate entry trajectory estimation.

Initially three tasks were defined. The first task was essentially to scope the problem by defining, in an error analysis sense, the expected delivery accuracy of the probes at entry. The results of this task are presented in Section II. The second task was an actual simulation task to provide for an accuracy assessment of the reconstruction process using appropriate models of the Earth based Doppler and on-board accelerometry. Nominal entry parameters assumed are given in Section III. The initial entry simulation efforts were conducted using a concept similar to that employed for the Viking lander trajectory reconstruction (Ref 1). In many instances, principally due to the lack of gyro data, this method was not entirely suitable. Thus the second task was modified to provide for a parallel development of an entry reconstruction method. This entailed the modification of the Viking Radio Science Software (VRSS) here at LaRC. Section IV of this report provides for a general discussion of the two methods and presents the results for the modified Task II. The influence of data drop-outs, quantization, and spacecraft and atmospheric modelling errors on both methods is discussed.

Section V of this report discusses the data pre-processing requirements. The Doppler data would be processed in the same manner in both concepts, i.e., used to update the spacecraft estimate, even though the filtering algorithms differ. However, the use of the accelerometry data in the two schemes is entirely different. The Viking scheme integrates the accelerometry deterministically to predict the spacecraft state. The conventional batch determination uses these data as external observables, not unlike Doppler, to enable updates for the state and environmental parameters. Wagner (Ref. 1) suggests

an alternate method which similarly models the aerodynamic forces and thus permits the use of the sensed accelerometry as observations to refine spacecraft and model parameter estimates. In Ref. 2 Sabin discusses a concept which could permit processing accelerometry data for improved estimation since the measurements are not required for prediction (as in his Mode A).

The third task in this contract was, based on the results of Task I and the modified Task II, to recommend the appropriate strategies and identify the required software for processing the multiple Venusian probes data. This report delineates the recommended procedures felt to be most applicable for Pioneer. Moreover, a summary of all the results obtained under this contract are presented as supporting data for the recommended process.

II. ENTRY NAVIGATION UNCERTAINTIES (TASK I)

Early efforts under this contract involved approach navigation error analyses to define a reasonable level of navigation accuracy for the probes at the entry interface as required by Task I. The results were generated using two programs which were originally developed by AMA, Inc. under the Viking Support Services Contract (NAS1-9100). The two programs used were the Viking Trajectory Generator (VTG) and the Parametric Orbit Determination (POD) Program. The VTG generates an appropriate reference conic given a launch and encounter date and a set of targeting specifications. POD performs a linear navigation error analysis using the VTG defined hyperbola as the reference spacecraft ephemeris. POD requires input to define the tracking schedule as well as the a priori uncertainties in the spacecraft state, dynamical and observational parameters. All Mars peculiar logic was modified for a Venus encounter. The targeting scheme in the VTG was modified to target to an impact point on the planet surface. An analytic planetary ephemeris was already available in both programs. (Ref. 3)

The assumed launch and arrival dates incorporated in the VTG were August 15, 1978 and December 10, 1978, respectively. The target impact point was defined in an Ecliptic of Date reference with the X-axis coincident with the sub-Earth point. The selected impact point was:

Latitude:	15^{o} N
Right Ascension:	2^{o} E

The resultant approach hyperbola was assumed representative for the probes, i.e., the actual probe release was not modelled. Approach statistics were generated along the reference conic to define a typical probe accuracy. Two assumed tracking profiles were considered. The nominal plan assumed all probes to be powered-up twenty (20) minutes prior to entry. The second profile, considered as an anomolous occurrence, assumed the probes to be "dormant" from separation until the entry interfaces. Neither the nominal nor anomolous separations were

included herein. The model simply mapped the bus covariance for 20 days. Statistics were also generated for the probe bus at entry assuming continuous tracking.

Ephemeris errors and central mass were modelled as dynamic consider parameters. Station locations uncertainties were modelled as observational consider parameters. Table II-1 of this report gives the assumed uncertainties used for the above consider parameters.

Entry accuracies obtained are as follows:

TABLE II-2 APPROACH COVARIANCE ANALYSIS RESULTS

	σ_v (mps)	σ_γ (deg)	σ_h (km)	σ_ψ (deg)	σ_φ (deg)	σ_λ (deg)
PROBE BUS	0.7	0.02	1.0	0.25	0.09	0.12
PROBE/DORMANT	1500	5.8	2063.	12.0	7.4	8.0
PROBE (20 MIN ARC)	3.2	0.05	5.0	0.95	0.35	0.42

These data were generated with Earth based range-rate data modelled to emulate Doppler data. An assumed accuracy of 1 mm/sec (for a 1 minute count time) was doubled to simulate appropriate 1-way noise. Appendix A of the report discusses the Doppler noise models and indicates this accuracy level may not be achievable in 1-way data since the spec value on the oscillator stability is only 1 part in 10^9. Therefore, the quoted statistics may be somewhat optimistic for the small probes. The probe bus and the large probe will be tracked with 2-way Doppler and the quoted statistics are felt to be quite reasonable. Approach statistics were generated for the small probes using the more conservative Doppler noise model (300 mm/sec noise level). The state uncertainties obtained were: σ_v = 11 mps, σ_γ = 0.2 deg, σ_h = 15.2 km , σ_ψ = 3.0 deg, σ_φ = 1.1 deg, σ_λ = 1.4 deg. The two sets of approach statistics obtained for the 20-min tracking arc were adjusted somewhat in defining "best" and "worst" case a priori uncertainties for subsequent entry covariance analyses. The "adjusted" statistics are given in Sec. III. In adjusting the statistics velocity

and flight path angle uncertainties were increased to provide some additional conservatism. Angle uncertainties (ψ , φ and λ) were rounded up to the nearest 0.5 deg level.

It will not be necessary to process the approach Doppler data here at LaRC since the JPL will provide state and covariance information to the entry science investigators at the entry interfaces ($\sim$200 km altitude). This part of the study was only undertaken to scope the entry reconstruction problem by defining a statistically probable range of entry flight path conditions to be expected.

PROBE A PRIORI (EE'50)

Position	σ_x	10,000 km
	σ_y	10,000 km
	σ_z	10,000 km
Velocity	$\sigma_{\dot{x}}$	1 km/sec
	$\sigma_{\dot{y}}$	1 km/sec
	$\sigma_{\dot{z}}$	1 km/sec

VENUSIAN EPHEMERIS UNCERTAINTIES (EE'50)

Position	σ_x	100 km
	σ_y	100 km
	σ_z	100 km
Velocity	$\sigma_{\dot{x}}$	10 m/sec
	$\sigma_{\dot{y}}$	10 m/sec
	$\sigma_{\dot{z}}$	10 m/sec

VENUSIAN MASS UNCERTAINTY

$\sigma_{\mu_{\varphi}}$ 1 km^3/sec^2

CYLINDRICAL TRACKING STATION LOCATION UNCERTAINTIES

σ_{rs}	1.5 m	, spin-axis
σ_{λ}	3 m	, longitude
σ_z	15 m	, z-height

TABLE II-1

INPUT UNCERTAINTIES FOR APPROACH COVARIANCE ANALYSIS

III. NOMINAL ENTRY PARAMETERS

For the ensuing analyses the following entry flight conditions were assumed:

TABLE III-1 NOMINAL ENTRY CONDITIONS AND UNCERTAINTIES

Parameter	Value	Uncertainty (1 σ)	
		LAS & Best Case SAS	Worst Case SAS
Velocity , V	11000 mps	5 mps	15
Flight path angle, γ	-38 deg	0.17 deg	0.25
Altitude, h	150 km	5 km	15
Heading, ψ	90^o	1.0 deg	3.0
Latitude, φ	0^o	0.5 deg	1.5
Longitude, λ	0^o	0.5 deg	1.5
Time of Entry	12/10/78 $0^h0^m0^s$(ET)		

The nominal trajectory is plotted in Figure III-1. Showed thereon are the velocity, flight path angle, altitude and axial acceleration for the first 20 seconds of the entry. This segment essentially covers the high speed dynamic region. The total flight time to impact is approximately 1 hour. Most of the ensuing analyses for the entry phase are concerned with this upper entry segment.

Model parameters assumed were as follows:

Spacecraft Parameters

Ballistic coefficient , $W/C_D A = 171 \text{ kg/m}^2$

in which, $C_D = 1.05$ (hypersonic) was assumed (see Fig. III-2). In some of the simulations the drag coefficient was changed to 0.8 to model the subsonic flight. In all cases $C_L \equiv 0$ was assumed.

Venus Parameters

$$GM_{\varphi} = 324858.77 \text{ km}^3/\text{sec}^2$$

$$R_{\varphi} = 6050 \text{ km}$$

The nominal atmosphere assumed was Model I of Ref. 4 which was based on the assumptions of most probable molecular mass and mean solar activity.

The orientation of the Venus equator in the EE'50 reference system was that defined in Ref. 5.

The JPL Development Ephemeris, DE96, was used for the VRSS simulations (Ref. 6).

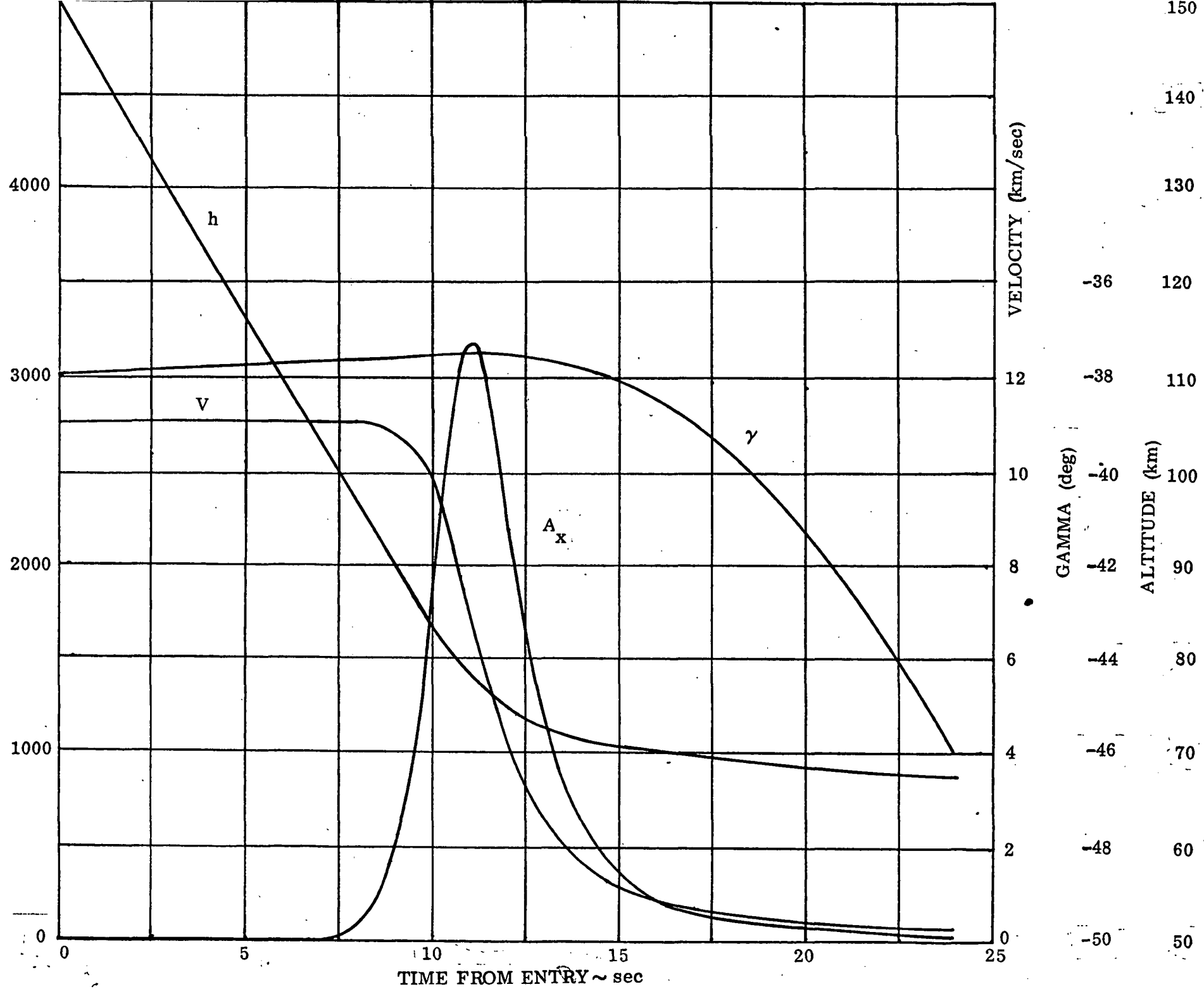

Fig. III-1 TYPICAL P/V ENTRY PROBE TRAJECTORY

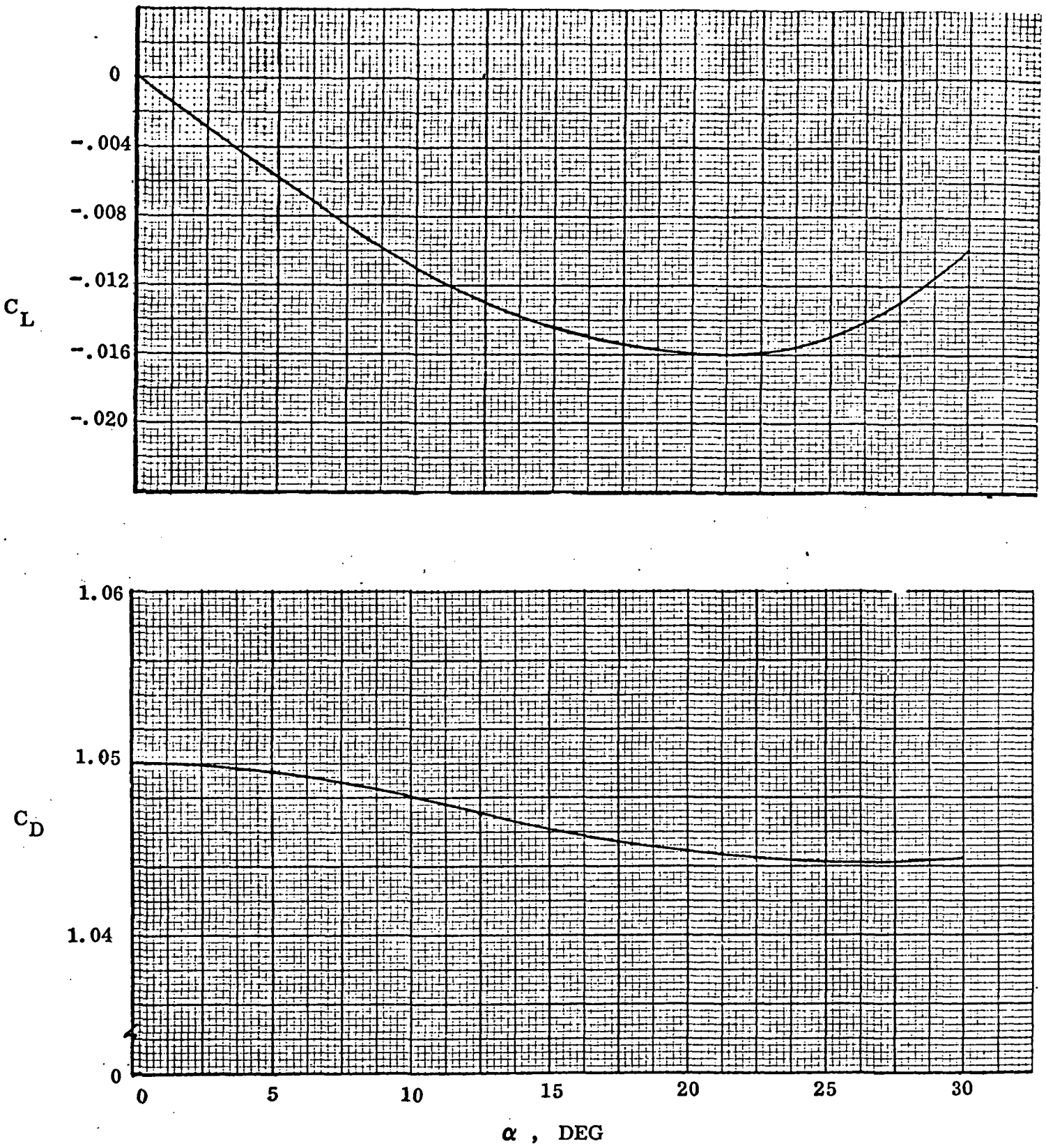

Fig. III-2 HYPERSONIC C_L AND C_D vs. α FOR P/V PROBES

IV. ENTRY RECONSTRUCTION METHODS (TASK II)

Two methods were considered for applicability to the Pioneer Venus multi-probe mission. The methods were:

(A) a Viking deterministic concept,

and (B) a conventional batch orbit determination method.

The principal difference between these two concepts is the nature in which spacecraft predictions are derived. There are other differences, e.g., the Viking technique employs a sequential Kalman-Schmidt consider algorithm and the VRSS obtains a batch Bayes estimate. However, of primary significance is the different state prediction methodology. The Viking concept integrates the accelerometer and gyro data deterministically to achieve spacecraft prediction, modelling only the additive gravity terms. Since these data are measured quantities the concept is essentially independent of atmospheric and spacecraft modelling. The VRSS achieves spacecraft prediction by a conventional Cowell integration in which the accelerations are computed based on some a priori model. Therefore this method is model dependent. However, since the measured spacecraft acceleration data are not utilized for prediction these data can be processed as external observables in concert with the Doppler data to update both the spacecraft state and atmospheric parameters. (A similar alternative is available using the alternate methods proposed as STEP1 and MODE B in Refs. 1 and 2, respectively). Therefore, the purpose of this task was to resolve a fundamental quandry; namely, is a simplified Viking technique feasible for Pioneer Venus sans gyros or is a more conventional orbit determination method more suitable, eventhough such a scheme is subject to a priori modelling errors.

IV.A. THE VIKING DETERMINISTIC METHOD

IV.A.1 Discussion and Results

The Pioneer Venus entry trajectories can be reconstructed using a Viking type technique under the basic assumption that the alignment of the spacecraft (more importantly the accelerometry) is known with respect to the planet relative velocity vector. This alignment assumption presumes each of the following:

(1) the spacecraft trim characteristics are predictable;

and, (2) there are no atmospheric winds present.

The alignment assumption is required in the absence of gyro data.

A simulation study was undertaken to determine the feasibility of the Viking deterministic method for Pioneer Venus entry reconstruction. The preceeding restrictive assumptions re atmospheric winds and spacecraft attitude were evoked. A nominal trajectory and associated range-rate and acceleration time history were generated. The initial conditions were offset and range-rate data processed to obtain trajectory estimates, predicts of course derived by deterministically integrating the nominal spacecraft acceleration data.

Figures IV-1 through IV-4 show actual state difference time plots for some of the simulation cases investigated. Plotted are velocity, altitude and flight path angle deviations from the ideal reference trajectory vs. time. Two curves can be seen on each figure. One curve shows the state differences during the forward pass. The jump discontinuities evident occur during the forward pass and are the necessary filter corrections required to fit the range-rate data. The other curve shows the differences during the backward smoothing pass which simply integrates the best estimate, based upon filtering throughout the forward pass, back to the nominal time of entry. Only V, γ, and h were estimated in this analysis. The corrections to the remaining state parameters were suppressed via a priori covariance input.

The results in Figure IV-1 were based on a modelled initial velocity error of 5 mps. Figure IV-2 shows the recovery characteristics using the deterministic scheme given an initial altitude estimate error at entry of 5 km. An initial flight path angle error was also modelled ($.17^{o}$) and the ability to reconstruct this type error is shown in Figure IV-3. A combined offset case is presented as Figure IV-4. Here all three of the important in-plane state parameters were initially in error at their respective 1σ levels. In all cases the corrections to the other state elements were suppressed via input a priori.

These cases were all the result of processing a 40 sec arc of range-rate data (to simulate Doppler) with a 10 sec blackout period near peak g. Simulation studies for longer arcs ($\sim$ 140 secs) exhibited serious convergence problems although solutions for the short 40 sec arc are by no means inconsequential since essentially the entire upper altitude high speed region of the entry is covered.

Clearly the results presented show that rapid convergence to the proper (albeit simplistically simulated) solution is achieved. Each of the important in-plane parameters are separable.

It is emphasized that these data were obtained by evoking the zero (or known) angle-of-attack history and no atmospheric winds were present. Also, it must be pointed out that the cases simulated made no attempt to constrain the accelerometry to the actual Pioneer data rate nor was any quantization error considered. Even with these nearly perfect conditions a pitch attitude error case was simulated but the results showed extreme divergence. It is felt that the zero (or known) assumption on spacecraft attitude is a reasonably good approximation in the absence of atmospheric winds. However prevalent winds at the upper altitudes (estimates are on the order of 100 mps) cannot be disregarded. If known they could be accounted for in the deterministic scheme.

IV. A. 2 Potential Use of the Viking Method

A technique to obtain a first-order density update using the Viking concept is discussed in Ref. 7. The method incorporates the in-situ accelerometry in the deterministic scheme to predict spacecraft state. Barometric altitude data derived by the Atmospheric Structures Experiment Team from the spacecraft pressure and temperature measurements would be used to shift the spacecraft altitude estimate. If the altitude were properly adjusted the density could be computed during the backward smoothing pass and these values of density would serve as the a priori model for the conventional orbit determination processor.

The basic assumption is that erroneous altitudes (deterministically predicted) are essentially dependent only on initial entry altitude errors. Given some pseudo altimetric fix (from the pressure and temperature data) this initial error can essentially be biased out to obtain the appropriate vertical profile for the backward pass. It was shown that initial velocity and flight path angle errors do not significantly introduce altitude error in the deterministic prediction scheme. Nor do reasonable pitch attitude ($<2^{o}$) errors contribute significantly. Therefore the procedure essentially shifts the altitude to the derived level and is "open-loop" in terms of the other state parameters.

Some rather large entry errors were considered in the accuracy analysis presented in Ref. 7. It was concluded therein that the simple method could conceivably yield density estimation accurate to within 10%. However, adverse combinations of the initial entry errors or erroneous datum shifts in the derived altimetry can completely destroy the reconstructed density accuracy.

Not considered in this analysis were either quantization effects or atmospheric winds.

IV. B. THE BATCH ORBIT DETERMINATION METHOD

IV. B. 1 Discussion

Task II of this contract was the performance of an entry reconstruction accuracy analysis using appropriate Doppler and accelerometry models to include both atmospheric and aerodynamic parameters as error sources. Because of the restrictive assumptions required to render the Viking concept useful as the multi-probe reconstruction tool, Task II was modified. The modification basically provided for a parallel development and evaluation of a completely different concept. The Viking Radio Science software, a batch orbit determination program which incorporates a Bayes estimator, was adopted as the baseline software. Appendix B of this report provides a discussion of the VRSS software used to perform the entry reconstruction task.

The accelerometry data were incorporated as observables. These data, which are used deterministically in the Viking concept for prediction, are not otherwise required in the batch concept. However, it is apparent that these in situ measurements contain significant information which can be gainfully employed in the reconstruction process. Whereas spacecraft prediction in this batch method is dependent on aerodynamic and atmospheric modelling parameters, it was felt that the mutual processing of both Doppler and accelerometry would aid in the resolution of any ambiquities. Consider for the moment an angle-of-attack error and its influence on the two observables. Since the probe aerodynamics (modelled as drag only) are independent of α the spacecraft trajectory, in a conventional integrator, is unchanged. Thus the Doppler shift is completely insensitive to this error. However, since the spacecraft x-axis is not in boresight alignment with the velocity vector the entire drag acceleration

is not sensed (cosine projection). Therefore combined Doppler and accelerometry processing could resolve this difference.

Atmospheric winds were added to the trajectory model to evaluate the effects of winds as modelling errors on the reconstruction process. A percentage change in the ballistic parameter, $C_D A/2W$, was used equivalently as a constant scale factor multiplier to provide for a model error implementation of atmospheric density. This was done to make use of the modelling available in the VRSS software.

IV. B.2 RESULTS

IV.B.2.1 Covariance Analysis

Covariance analyses for both the large and small P/V probes have been performed using Doppler and accelerometer data over an arc from Entry to Entry+40^s. The probes are equipped with both velocity-counting (ΔV) and instantaneous acceleration sensors, and these were treated as separate data types in the analyses. The large probe has 2-way Doppler, while the small probes have 1-way Doppler. Since the accuracy of 1-way Doppler is somewhat speculative, small probe covariance results were obtained using "best" and "worst" case 1-way accuracies. Thus, a total of six (6) cases were required to represent the possible combinations of data types and data accuracies.

A discussion of the noise models used for the Doppler and accelerometer data types is given in Appendix A. The data coverages for each measurement type are as follows: (1) Doppler (1,2-way) data at 1/sec, with data loss from E+8^s to E+16^s due to blackout; (2) ΔV derived accelerometry data at 4/sec; (3) Instantaneous acceleration data at 1 per 2 sec. The solution parameter set consisted of S/C state (V , γ, ψ , R , φ , λ) and the ballistic coefficient C_D' ($C_D A/2W$), which has been interpreted as a density scale factor and is presented as a percentage accuracy in the density (ρ). Angle of attack (α) , which could have been used in the solution parameter set for accelerometry only and combined Doppler and accelerometry, was assumed known perfectly.

Covariance results for the large probe are given in Table IV-1. Results for the small probes based on best and worst case 1-way Doppler accuracies are

shown in Tables IV-2 and IV-3. Only optimal statistics were generated, i.e., contributions due to uncertainties in either observational or dynamic parameters (not solved-for) were not reflected in the statistics. Therefore the results are only influenced by data quantity, assumed data accuracy, and a priori uncertainties used.

The following remarks are pertinent to all cases considered. The parameters ψ , φ , λ are not "observable" in the accelerometry data, whereas the Doppler (range rate) data contains some information for all 7 solution parameters. (See Appendix C). Furthermore, accelerometer data is continuous (no dropouts due to blackout), while the significant information content contained in the Doppler data near peak g is lost due to blackout.

The results for the large probe (Table IV-1) indicate a significant reduction from the apriori values for γ , h , λ , and ρ with a moderate reduction ($\sim 50\%$) in the V uncertainty due to Doppler processing only. A slightly better determination of V is obtained using instantaneous accelerometer data and excellent statistical determination of all seven parameters is obtained using Doppler and the instantaneous accelerometry combined.

Table IV-2 shows the best case covariance results for the small probes. The accelerometer only results are identical to those obtained for the large probes. Doppler and Doppler combined with accelerometry yield essentially the same results as those obtained for the large probes since the 1-way Doppler data are considered almost as accurate as 2-way. These results are considered optimistic for the small probes.

Worst case 1-way Doppler results for the small probes (Table IV-3) indicate potential problems in accurate entry reconstruction unless instantaneous accelerometer data are used (and with accuracy comparable to that assumed in this report). As shown in Table IV-3 the a priori uncertainties are rather large, since they were based on "inaccurate" 1-way Doppler data for the 20 minutes prior to entry. Neither the Doppler nor ΔV-derived accelerometry data can significantly reduce the uncertainty in entry velocity. However, the results obtained with the instantaneous accelerometer data alone not only represent reasonable state determination but also are almost independent of the a priori for those parameters which are determinable (V , γ , h , and ρ).

As shown in Appendix A, the instantaneous accelerometers are assumed exceedingly accurate and always yield better results than the velocity-counting accelerometers even with the limitation of only 1/8 the data quantity. The ΔV derived accelerometry cannot be considered more accurate due to the high quantization levels indicated in Appendix A. The large quantization noise, specifically during BLACKOUT II, which must be accounted for tends to diminish the information content in the observable. The elapsed time in which the sensors are in this Mode is rather lengthy considering the short peak g pulse duration. Consequently, over much of this interval the signal to noise is quite small as shown in Fig. IV-5. Throughout the entire 40 sec arc the noise is less than 1% of the signal for only 1.5 seconds. In fact, the noise exceeds 10% of the signal 30% of the entire interval. It is hard to quantify that level of SNR which is sufficient but it has been shown that even with the large quantization noise very good γ, h, and ρ estimation is possible.

IV. B. 2.2 Simulations

The applicability of the conventional orbit determination technique to entry reconstruction was initially shown by demonstrating the ability of the process to recover initial condition errors using Earth-based Doppler data only.

The four modelled offset cases which had been used in evaluating the deterministic scheme were utilized. These were: (1) $\Delta V_0 = 5$ mps; (2) $\Delta\gamma_0 = .17$ deg; (3) $\Delta h_0 = 5000$ m; (4) ΔV_0, $\Delta\gamma_0$, Δh_0 combined. In each case the offsets represented expected 1σ uncertainties in the appropriate parameter(s). Six (6) component state only solutions were obtained for the first three cases using Doppler data at 1/sec over the arc Entry to Entry $+40^S$. Loss of Doppler data due to blackout was not considered. All solutions were obtained with the same a priori constraints used for the deterministic scheme.

Table IV-4 contains results for the three offset cases. The convergence characteristics of the batch process are illustrated by showing the errors in individual state components after each iteration. Another indicator of convergence, the weighted root mean square of the Doppler residuals (rms_W) is also given. A value of 1 for rms_W means that the data have been fit to the assumed noise level (2 mm/sec, the value used with the deterministic scheme). Since the Doppler

data used in these cases were modelled (unrealistically) noise-free, perfect recovery of the initial condition errors is possible ($rms_W = 0$). At least 4 iterations are required to remove the initial condition error modelled for each case. The over-correction tendency of the process, particularly in the early iterations, is due to the extreme non-linearities occurring around peak g. However, at no time do the solutions appear to be diverging since rms_W is always decreasing.

After the development of the accelerometer data processing program, PVETNA (see Appendix B), the combined V , γ, h offset case was used to evaluate filter performance. Since there is no information in the accelerometry for ψ , φ, λ , a 3 component (V , γ, h) state solution was obtained using instantaneous accelerometer data at approximately 4/sec for the arc Entry to Entry $+40^S$. It was assumed that accelerometer data would be available near peak g.

Table IV-5 contains the results for the combined V , γ, h offset case. Convergence characteristics are again illustrated by showing the errors in individual state components after each iteration. The peak-to-peak spread and the weighted root mean square (rms_W) of the residuals are also shown. The assumed accuracy of the accelerometer data used in computing data weights and rms_W was 0.1% of the measured value. The accelerometer data, however, were noise-free. Also shown in Table IV-5 are 3-components (V , γ , h) state solutions obtained using Doppler data only, both with and without blackout. The assumed accuracy of the Doppler data for these cases was 15.5 mm/sec.(1)

As shown in Table IV-5, the initial condition errors produce excessive first pass residuals for both data types (the maximum residuals occur near peak g). Therefore, it is not surprising that many iterations are required to remove the initial condition errors for the accelerometer and no-blackout Doppler solutions. For the Doppler solution with blackout, the first pass residuals are much more reasonable, since the large residuals occurring near peak g (and much of the information content) have been excluded. However, the information content in the remaining data is sufficient to achieve convergence in 2 iterations.

(1) 2mm/sec accuracy adjusted for the 1 sec count time (see Appendix A)

IV. C. PROBLEM AREAS

This section discusses various problem areas which can affect the multi-probe reconstruction process. In each case the problem will be discussed as to its relative importance on the two reconstruction methods since, in most instances, it can represent an entirely different phenomenon. The following problem areas are discussed:

(1) Spacecraft modelling
(2) Data drop-outs
(3) Data Rates
(4) Quantization
(5) Atmospheric Density
(6) Atmospheric Winds

IV. C.1 Spacecraft Modelling

Spacecraft modelling, as discussed herein, includes the following:

(1) aerodynamics,
(2) mass properties,
and (3) attitude.

The hypersonic aerodynamic characteristics of a typical probe were presented in Fig. III-2. It can be seen that the drag only model employed in the conventional method is a very good approximation. Further, there is little variation in the aerodynamics for reasonable excursions in α. Obviously any inaccuracy in these data will affect spacecraft prediction in the conventional integrator. Efforts should be made to incorporate variations with Mach No. in the conventional integrator. The deterministic method is insensitive to C_D errors except any derived density information cannot be considered more accurate than the drag is known.

The current density (or C_D) scale factor term employed in the VRSS software is a collective "sink" for the spacecraft model. The covariance analysis discussed previously indicates this parameter is determinable to within 4.6% even with the worse case measurement model. A known 10%

error in this "collective parameter" was recovered via simulation. Clearly, this parameter, if incorporated separately, will be high correlated with any density model employed. Hopefully, a realistic density model, one which varies with altitude, is separable from this constant term since the processing arc does encompass many scale heights. It is conceivable that the pre-flight ballistic parameters are sufficiently well known to preclude this term as a solution parameter. It is also conceivable that the Atmospheric Structures Experiment Team might well choose to determine two drag parameters--a supersonic and a subsonic scaling factor.

The initial spacecraft mass, and predicts to account for mass loss due to ablation, are assumed known. Again, errors in these parameters will affect prediction in the conventional integrator and the derived density accuracy via the deterministic scheme.

Because there are no gyros spacecraft attitude must be prescribed in the deterministic integrator in the same manner as required in the conventional integrator, i.e., some a priori trim estimate must be assumed. Use of an attitude time history derived from a six-degree-of-freedom simulation has been suggested. (2) There exists no ability to solve for spacecraft attitude in the deterministic mode without gyros. The assumption of alignment of the accelerometer(s) with respect to the relative velocity vector is a reasonable approximation if there are no winds present. Any attitude deviation away from zero (boresight alignment with the velocity vector) results in a sensed loss of the total drag deceleration actually imparted to the spacecraft. A 1^{o} residual error in the orientation can induce an approximate 1 mps accumulated velocity loss compared to the actual. An attitude error of 2^{o} would result in a sensed velocity error approximately 3.6 mps less than the actual. These errors appear early in a deterministic entry prediction, i.e., immediately following peak g, and induce horrendous prediction errors for longer integration time. One must keep in mind that the actual velocity decrement undergone at the spacecraft is

(2) Appendix E shows a typical probe attitude profile and discusses the implications when the known attitude is neglected (or that assumed in error).

independent of angle-of-attack. Thus, in a deterministic scheme the sensed ΔV (converted to acceleration) must be properly adjusted to account for a non-aligned sensor/velocity orientation.

Since the aerodynamics are not strongly dependent on spacecraft attitude the predicted trajectories are unaffected for the conventional integrator. However, the conventional reconstruction scheme is not entirely independent of attitude knowledge since the measured accelerations which are processed as observational data are certainly affected by sensor deviations from the drag direction. Since the trajectory is unaffected an apparent inconsistency occurs between the measured ΔV and the Doppler. Combined data processing should enable the determination of such an ambiguity.

Clearly if atmospheric winds are present the preceeding statements re attitude are invalid. Winds must be known to properly prescribe the spacecraft attitude. Since there is no source for winds throughout the upper entry segment, they must be solved for. A layered technique in which the winds are modelled as constant parameters to be estimated within a given layer, should be employed.

IV. C. 2 Data Drop-Outs

Doppler data is expected to be lost near peak g since blackout will occur. Accelerometry data during blackout are recorded and played back during the descent, interleaved with the on-going measurements. No loss of accelerometry information is expected.

If any acceleration data are lost during the peak g interval it will make it extremely difficult, if not impossible, to obtain a reasonable deterministic prediction. A similar loss of data will not significantly affect the conventional scheme since these data are not used for prediction. The data drop-out would simply reduce the number of acceleration observables for processing. Of course, both methods are compromised if the entire peak g interval ($\sim$8 - 14 secs) is lost. In this event the deterministic scheme would be rendered useless. The conventional scheme would only have Doppler observables available for processing (since the relevant information in the accelerometry occurs during the peak g interval) and it is known that certain parameters are observable only when the combined data types are processed.

The loss of Doppler due to blackout, which occurs near peak g, has been shown to be of no major consequence. Admittedly the maximum sensitivity of Doppler to the solution parameters occurs near peak g. However, the non-linearities therein produce some large erroneous updates in the conventional scheme which increases the number of required iterations for convergence. Loss of Doppler entirely, or data rendered useless for some unforseen reason, would be catastropic for both schemes. The deterministic scheme integrates the other observable (accelerometry) for prediction. There would be no additional data (apart from any derived pseudo altimetric information) to update these predictions and elimate the initial trajectory errors. In the conventional scheme, if all Doppler data are lost, the solutions obtained by processing accelerometry only would be limited. All the solution parameters are not observable in accelerometry alone. Moreover, those parameters felt to be observable by the combined processing technique would be indeterminable.

IV. C. 3 Data Rates

There are no conceivable problems with the current data rates for the conventional scheme. Doppler data at 10/sec during the upper entry segment and 1/sec during the long vertical flight are achievable and certainly acceptable. Accelerometry data are available at 0.25 sec intervals--derived from the ΔV pulse counts. Instantaneous accelerations at 2 second intervals during blackout (and less frequently during the TRANSITION phase) are also available for processing. These data, though less frequent, are considered to be far more accurate ($\sim$.1 g or better).

The Doppler availability represents no problem for the deterministic scheme. However, the frequency of the accelerometry data poses some problems in the deterministic scheme. At a data spacing of 0.25 sec, even with perfect accelerometry, it was difficult to obtain good nominal deterministic prediction. Large local errors in velocity occurred near peak g since the limited data rate did not entirely prescribe the peak g pulse. Moreover, a residual hang-off

velocity error occurred after the pulse and this error, even though on the order of 0.1 mps, caused rapid divergence when integrated for longer trajectory times. The deterministic scheme is inherently unstable because the velocity error in near vertical flight induces altitude errors which in turn produce different gravity effects. This then increases the velocity differences, etc. Unlike the deterministic integrator the conventional integrator, for a range of initial condition errors, tends to converge to the same final vertical flight conditions after approximately 100 sec since the accelerations are computed quantities at altitudes. The accelerations for the deterministic integrator, simply a function of time, are independent (at the predicted altitude) of any assumed density-altitude profile. Moreover the values required at the half-intervals for the 4th order Runge-Kutta scheme employed are interpolated values. Much effort was expended to try various higher order interpolations to obtain better velocity comparisons near peak g and ultimately eliminate the hang-off error. Whereas some improvement was obtained the results still were not satisfactory.

A more sophisticated observable was modelled to emulate the actual spacecraft acceleration measurement. Actual accelerations at a very fine step size (0.005 sec) were accumulated using a simple trapezoidal integration. The resultant output was then a time function of the total ΔV accumulated at the 0.25 sec spacing. The fine structure of the accumulated ΔV is inherently embedded in these data. A cubic spline derivative routine (See Section V-B) was used to operate on these data to back out the fine structure. Equivalent accelerations, spaced at a 0.125 sec interval to eliminate interpolation, were output. The nominal prediction obtained was extremely good as shown in Fig. IV-6. The maximum velocity deviation occurring near peak g was 0.0025 m/sec. It is obvious that the cubic spline derivative routine resurrects the finer structure in the acceleration history though the data spacing of the input file is only 0.25 sec. There are however some deviations between the actual and derived accelerations near peak g but the total ΔV is preserved. The cubic spline derivative routine forces continuity through the second derivative, i.e., yielding continuous acceleration and jerk values (although the latter are not differentiable).

IV. C. 4 Quantization

Quantization of the spacecraft acceleration measurements is discussed in Appendix A. With quantization modelled the cubic spline routine tends to follow the noise. This output, as input to the deterministic process, is therefore the model and the deterministic integrator tracks the quantization noise. Thus a noisy, and rather large, velocity deviation from the reference trajectory occurs. The velocity prediction error between the deterministically integrated nominal and actual reference values are plotted in Fig. IV-7. Also shown are the differences between the actual accelerations and those derived from the cubic spline routine using the accumulated ΔV file with the additive quantization noise. In order to use the Viking method for Pioneer some smoothing of the actual data would be required to minimize the effects of the quantization noise. Figures IV-8 and IV-9 show comparisons in velocity and acceleration between the deterministic nominal and the reference values for two levels of smoothing: S = 10. and S = 100. (see Section V-B). Clearly the local velocity error near peak g increases as more smoothing is applied. However, the difference between the derived accelerations and the actual values decreases in magnitude as smoothing is applied. There is also noticeably less frequency content in the difference plots for increased smoothing, as expected. It must be noted that the entire 40 sec ΔV curve was smoothed and it is quite probable that better results could be obtained by breaking the file into smaller regions. A definite observation one can make is that the quantization effects, spread over some 13-14 secs of the entry flight because of the length of the BLACKOUT II mode, is restricted to a much shorter time span when smoothed.

The resultant influence of the quantization error on the accelerometry measurements for the conventional scheme was discussed in the preceding covariance analysis (Sec. IV. B. 2. 1). It was shown that eventhough the data are downweighted there is extant much information to enable the determination of velocity, flight path angle, entry altitude and density.

It is obvious that the quantization effects are more severe for the Viking type deterministic reconstruction technique. Fortunately, with or without

smoothing, the altitude prediction is very good for the 40 second arc. This fact is considered important because of the potential application of the Viking method discussed in Section IV.A.2.

IV.C.5 Atmospheric Density

The Viking deterministic method is insensitive to atmospheric density uncertainties. The actual density encountered is reflected in the in situ measurements of spacecraft acceleration. The conventional method is very dependent on a priori knowledge of the atmospheric density, as discussed in Appendix D. However, it may be possible to solve for the density since it is observable. The following discussion points out the dependency of the conventional scheme on density modelling errors and gives the rationale for the preceding conclusion.

A 10% density scale factor was simulated as an error source. One could consider this an erroneous drag estimate. For the purposes of discussion it is considered herein as a constant density scale factor error. Fig. IV-10 shows the resulting trajectory dispersions due to the constant 10% density scale factor. It can be observed by comparison with the figures in Appendix D that, apart from scale, an almost identical signature is obtained with the constant density error as is obtained with the models.

This known error, modelled as a constant, is readily determined when included in the solution set. However, with state only estimation, a large erroneous state update results. Two state only solutions were obtained with this error modelled. An accelerometer only and a combined radio and accelerometer solution were obtained. Data were processed during the first 40 secs only. The solutions obtained were as follows:

ACCELEROMETRY ONLY

ΔV = 111 mps

$\Delta \gamma$ = 0.29 deg

Δh = 534 m

$\Delta V = 19$ mps

$\Delta \gamma = 0.28$ deg

$\Delta h = 237$ m

Figure IV-11 shows the initial Doppler and accelerometer residuals which result due to the density scale factor error. The final residuals for the accelerometry only solution are shown as Fig. IV-12. Here the Doppler residuals are simply an indication of how well the accelerometry only solution fits the range rate data. Quite clearly neither data type is fit well. True the accelerometer residuals are essentially halved but the Doppler residuals are degraded considerably. Fig. IV-13 shows the final residuals for combined data processing. The range rate data appears to be fit reasonably well although there is still some signature remaining. Peak accelerometer residuals of $\pm$ 50 m/sec^2 certainly are not indicative of a reasonable fit. It is quite apparent that the entry state estimate cannot be aliased to absorb the density model error.

The converged solutions were mapped and compared versus the appropriate reference. These trajectory comparisons are shown as Figs. IV-14 and IV-15, respectively. Whereas the altitude differences are everywhere less than 1 km, there are large velocity and flight path angle deviations during the upper entry segment.

As stated previously, if the solution set were expanded to include the constant density term an exact solution would occur. Therefore, the density is observable. Whether both density and C_D (or some equivalent ballistic parameter) are separable is a question which needs be addressed. In the worse case, if not separable, the resultant density would necessarily need be defined with an appropriate uncertainty to reflect the uncertain spacecraft model parameters.

IV.C.6 Atmospheric Winds

Figure IV-16 of this report shows the trajectory deviation from the nominal trajectory due to a 100 mps East Wind. No cross track errors are introduced since this is a tail wind in the plane of the trajectory. The essentially steady-state velocity error which results is approximately 50 mps. The inertial flight

path angle is in error by approximately 60 deg eventhough the flight path angle of the velocity vector relative to the atmosphere is, of course, 90 deg. The spacecraft is essentially blown along by the wind but the vertical profile (altitude and altitude rate) is essentially unchanged due to the horizontal wind imposed.

Theoretically the Viking deterministic concept is independent of a priori modelling of all atmospheric parameters. It is of course affected by unknown misalignments, data drop-outs, biases and scale factor uncertainties in the inertial reference unit which measures in situ the "equations-of-motion". However, in the absence of complete accelerometry and without gyro data, the concept no longer enjoys the "model-free" distinction if winds are present.

In the deterministic scheme atmospheric winds reflect, in essence, spacecraft attitude errors.[3] The spacecraft is erroneously forced to some attitude with respect to the relative velocity vector (V_R) , for lack of gyro data or wind information, and the errors in the state grow divergently (Fig. IV-17). The existence of atmospheric winds would negate the simple first-order density scheme discussed in Sec. IV A.1. Eventhough the wind modelled was only a horizontal component an altitude error of $\sim$1.8 km occurs after 45 secs of prediction. Again this is due to the lack of gyro information and therefore, the restrictive assumption which needs be made re the spacecraft attitude. For Viking, information was fully contained in the gyro and accelerometry. The Viking inertial (and plant relative) reconstruction accuracies were independent of winds. However, the inertial attitude of the spacecraft was determinable from the integrated gyro data. Although the inertial trajectory parameters were recoverable it was evident by inspection that the computed attitude angles (α and β) with respect to V_R (since winds were presumed zero) were quite different than the pre-flight trim predicts. The full gyro and accelerometer data contained all the deterministic integrator need know about the winds. Use was made of the erroneous α and β to solve for the winds, given that the

(3) Indeed the magnitude of the acceleration will change also since V_R is not equal to the velocity of the spacecraft relative to the atmosphere when winds are present.

inertial spacecraft state were in fact valid. The pre-flight pitch attitude trim characteristics (with an assumed $\beta \equiv 0$) were processed as pseudo data to compute wind velocity and direction from the attitude residuals (Ref. 8).

The batch orbit determination concept is also very much affected by winds. There is some evidence that strongly suggests the winds are determinable in the conventional approach. This fact is simply derived from the Doppler signature. No other parameter produces a signature in the Doppler similar to that resulting from atmospheric winds, in particular, the residual shift which persists long past the peak g pulse. All other parameters, and all other modelling errors, converge to essentially the same terminal flight trajectory (though the altitude at this time may differ by several hundred meters for different density models). The Doppler sensitivities shown as Fig. C-6 through C-9 in Appendix C of this report all tend toward zero after approximately 20 seconds into the entry.

The effect of winds on the conventional approach was evaluated using "real world" accelerometer and range rate data containing the 100 mps wind, but processed using a mathematical model without winds. The errors in the mathematical model are shown in the accelerometer and range rage residuals obtained on the first pass through these data, i.e. prior to the fit. (Figs. IV-18). Whereas the accelerometer residuals tend to zero after the peak g period, the range rate residuals approach -60 mps. This characteristic of the range rate residuals suggests that winds are at least identifiable, if not completely determinable.

As stated, no other parameter, certainly not entry initial conditions, can produce such trajectory (and Doppler) mechanics. A state only solution with Doppler was attempted and, as expected, was grossly divergent. However, a 40 sec arc of acceleration data was processed. The solution obtained for this model error was as follows:

$$\Delta V = -71 \text{ mps}$$
$$\Delta \gamma = -0.29 \text{ deg}$$
$$\Delta h = 7 \text{ m}$$

Fig. IV-19 shows accelerometer and Doppler residuals for this solution. Since only accelerometry data were fit these are the final residuals for the converged state estimate. The Doppler (range rate) residuals are simply the differences between the measurements and computed values based on the converged accelerometry estimate. The Doppler residuals are actually worse than those obtained on the initial pass. Comparison of the acceleration residuals before and after the fit show an approximate order of magnitude reduction in the peak excursion. It would appear that the acceleration data were reasonably well fit. In particular, were the quantization noise modelled, the accelerometer residuals might well be entirely masked and the fit otherwise assumed good. However, it is the strength of the mutual data processing which yields the necessary wind information. If accelerometry data seem reasonably well fit, and further no solution can be achieved with Doppler, one can assume a very good first order indication of the existence of atmospheric winds. This alone does not yield sufficient information to determine the magnitude and direction of said winds. It is felt that winds, if added formally as solution parameters, are determinable. One should adopt an altitude varying model for the winds to provide for a physically motivated model.

The above solution, which may be considered as a "corruption" to the entry estimate, was mapped assuming no winds since winds were not used in the fitting process. This trajectory was compared versus the nominal with winds, assumed to be representative of the real world flight condition. Figure IV-20 shows these trajectory differences, again indicating that the state only estimate cannot compensate for an unknown wind.

A POSTERIORI STATISTICS @ ENTRY

PARAMETER	A PRIORI	DOPPLER[1]	$A_{\Delta V}$[2]	DOP&$A_{\Delta V}$	A_I[3]	DOP & A_I
σ_V (mps)	5	2.7	4.8	2.7	1.7	0.6
σ_γ (deg)	0.17	0.01	0.06	0.01	0.01	0.003
σ_ψ (deg)	1.0	0.7	1.0	0.7	1.0	0.6
σ_h (m)	5000	4	73	3	12	3
σ_φ (deg)	0.5	0.4	0.5	0.4	0.5	0.3
σ_λ (deg)	0.5	0.03	0.5	0.03	0.5	0.02
σ_ρ (%)	—	0.3	3.0	0.3	0.4	0.1
NPTS		31	167	198	21	52

NOTES:

(1) 2 - way Doppler data assumed

(2) $A_{\Delta V}$ .... derived accelerometry from ΔV pulses

(3) A_I ..... Instantaneous acceleration data

TABLE IV-1

COVARIANCE ANALYSIS FOR LARGE PROBE ENTRY RECONSTRUCTION

		A POSTERIORI STATISTICS @ ENTRY				
PARAMETER	A PRIORI	DOPPLER (1)	$A_{\Delta V}$	DOP &$A_{\Delta V}$	A_I	DOP&A_I
σ_V (mps)	5	3.4	4.8	3.4	1.7	0.9
σ_γ (deg)	0.17	0.02	0.06	0.02	0.01	0.005
σ_ψ (deg)	1.0	0.8	1.0	0.8	1.0	0.7
σ_h (m)	5000	6	73	6	12	5
σ_φ (deg)	0.5	0.4	0.5	0.4	0.5	0.3
σ_λ (deg)	0.5	0.03	0.5	0.03	0.5	0.03
σ_ρ (%)	—	0.6	3.0	0.5	0.4	0.2
NPTS		31	167	198	21	52

(1) Optimistic 1-way model derived from 2-way accuracy

TABLE IV-2

COVARIANCE ANALYSIS FOR SMALL PROBE ENTRY RECONSTRUCTION

(BEST CASE 1-WAY DOPPLER)

		A POSTERIORI STATISTICS @ ENTRY				
PARAMETER	A PRIORI	DOPPLER[1]	$A_{\Delta V}$	DOP+$A_{\Delta V}$	A_I	DOP+A_I
σ_V (mps)	15	13	12	10	1.8	1.8
σ_γ (deg)	0.25	0.17	0.07	0.07	0.01	0.01
σ_ψ (deg)	3.0	2.8	3.0	2.6	3.0	2.4
σ_h (m)	15000	79	73	24	13	12
σ_φ (deg)	1.5	1.4	1.5	1.3	1.5	1.1
$\sigma\lambda$ (deg)	1.5	0.2	1.5	0.1	1.5	0.1
σ_ρ (%)	——	4.6	3.0	1.9	0.5	0.5
NPTS		31	167	198	21	52

(1) Conservative 1-way model derived from oscillator instability

TABLE IV-3

COVARIANCE ANALYSIS FOR SMALL PROBE ENTRY RECONSTRUCTION

(WORST CASE 1-WAY DOPPLER)

	ΔV (mps)	$\Delta\gamma$ (deg)	$\Delta\psi$ (deg)	Δh (m)	$\Delta\varphi$ (deg)	$\Delta\lambda$ (deg)	rms_W (-)
V - OFFSET	5	0	0	0	0	0	19
ITER # 1	0.5	-7E-4	-5E-5	6	-2E-4	-7E-4	16
ITER # 2	-10	-1E-2	-4E-3	-50	-7E-4	-1E-2	10
ITER # 3	-5	-2E-3	3E-4	-20	5E-4	2E-3	2
ITER # 4	-0.1	1E-4	2E-5	-1	2E-5	1E-4	0.16
h - OFFSET	0	0	0	5000	0	0	3014
ITER # 1	-1000	-3E-1	8E-2	-8000	-2E-1	-2E-1	563
ITER # 2	-100	2E-2	2E-3	-600	7E-3	3E-2	92
ITER # 3	-3	5E-3	5E-4	-30	1E-3	5E-3	6
ITER # 4	-5	-2E-3	5E-4	-30	1E-3	-2E-3	2
ITER # 5	-0.1	-1E-4	2E-5	-1	2E-5	1E-4	0.14
γ - OFFSET	0	1.7E-1	0	0	0	0	8044
ITER # 1	-60	-3E-2	6E-3	-500	-2E-2	-3E-2	67
ITER # 2	3	7E-5	1E-4	20	-1E-4	-9E-6	18
ITER # 3	-10	-1E-2	-4E-3	-50	-8E-4	-1E-2	10
ITER # 4	-5	-2E-3	5E-4	-20	-1E-3	-2E-3	2
ITER # 5	-0.1	1E-4	2E-5	-1	2E-5	1E-4	0.16

TABLE IV-4

BATCH RECONSTRUCTION - INDIVIDUAL STATE ERRORS SIMULATED

(RANGE RATE DATA ONLY)

ACCELEROMETRY ONLY

				SPREAD ON RESIDUALS		
	ΔV (mps)	$\Delta\gamma$ (deg)	Δh (m)	$(O-C)_{MIN}$ (m/sec^2)	$(O-C)_{MAX}$ (m/sec^2)	rms_w (-)
OFFSET	5	0.17	5000	-1400	980	416
ITER # 1	104	3.71	-5923	- 243	210	674
ITER # 2	-456	0.24	-2864	- 322	319	159
ITER # 3	- 89	-0.04	- 469	- 52	2	9
ITER # 4	-2.5	+0.0004	- 14	- 2	2	0.7
ITER # 5	+0.5	+0.002	1	0	0.2	0.03

RANGE RATE ONLY

(NO BLACKOUT)

				(m/sec)	(m/sec)	
OFFSET	5	0.17	5000	- 6	2015	33500
ITER # 1	428	6.78	-8453	- 234	314	8100
ITER # 2	6	1.11	-1070	- 68	236	4537
ITER # 3	10	0.17	- 194	- 4	10	183
ITER # 4	0.2	0.004	- 5	———	———	———

(WITH BLACKOUT)

OFFSET	5	0.17	5000	- 6	133	2220
ITER # 1	- 22	-0.31	1260	- 1	16	250
ITER # 2	-0.05	+0.004	- 2	———	———	———

TABLE IV-5

BATCH RECONSTRUCTION - COMBINED STATE ERRORS SIMULATED

(RANGE RATE AND ACCELEROMETER DATA)

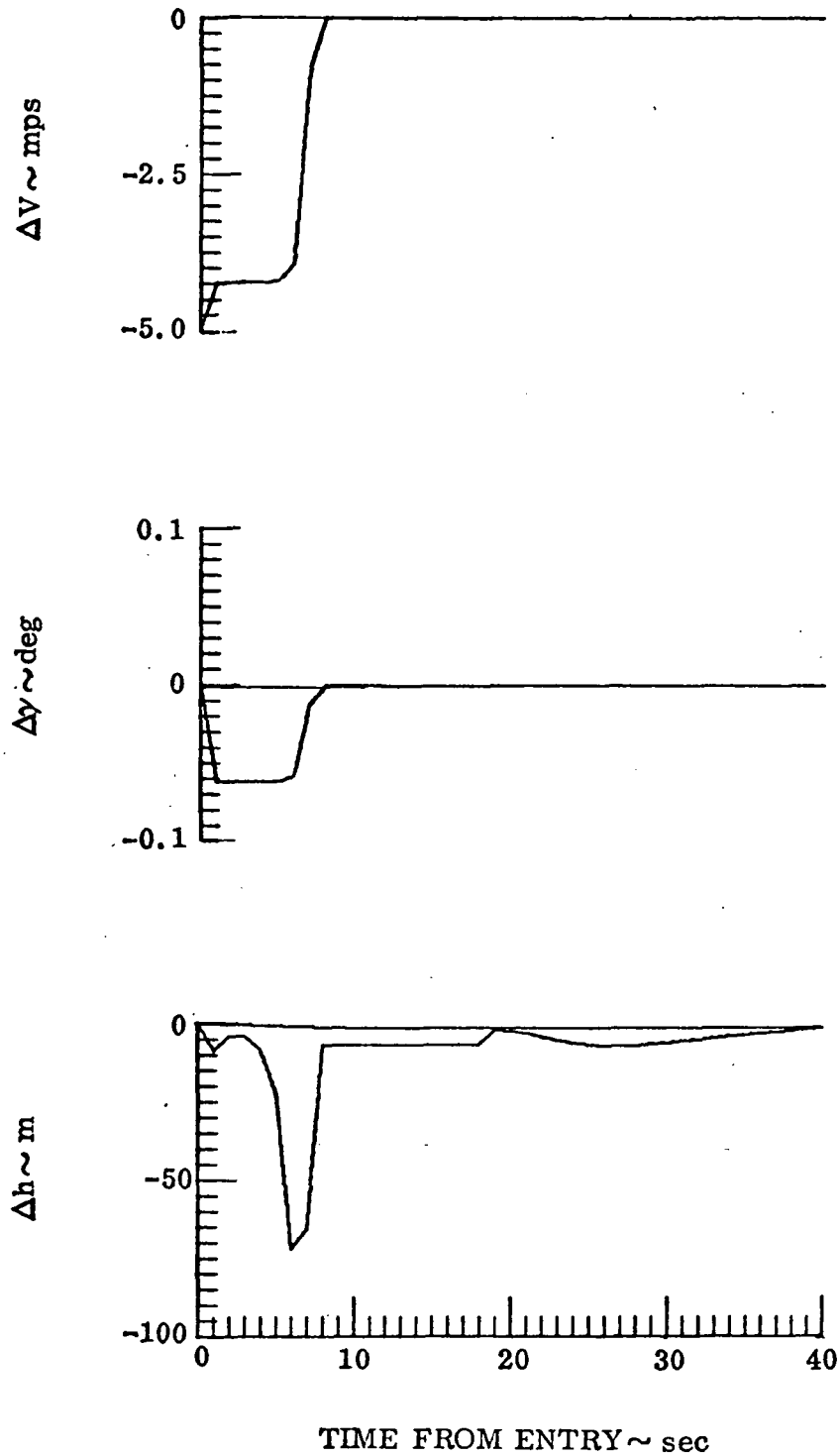

Fig. IV-1 DETERMINISTIC RECONSTRUCTION - INITIAL VELOCITY ERROR SIMULATED

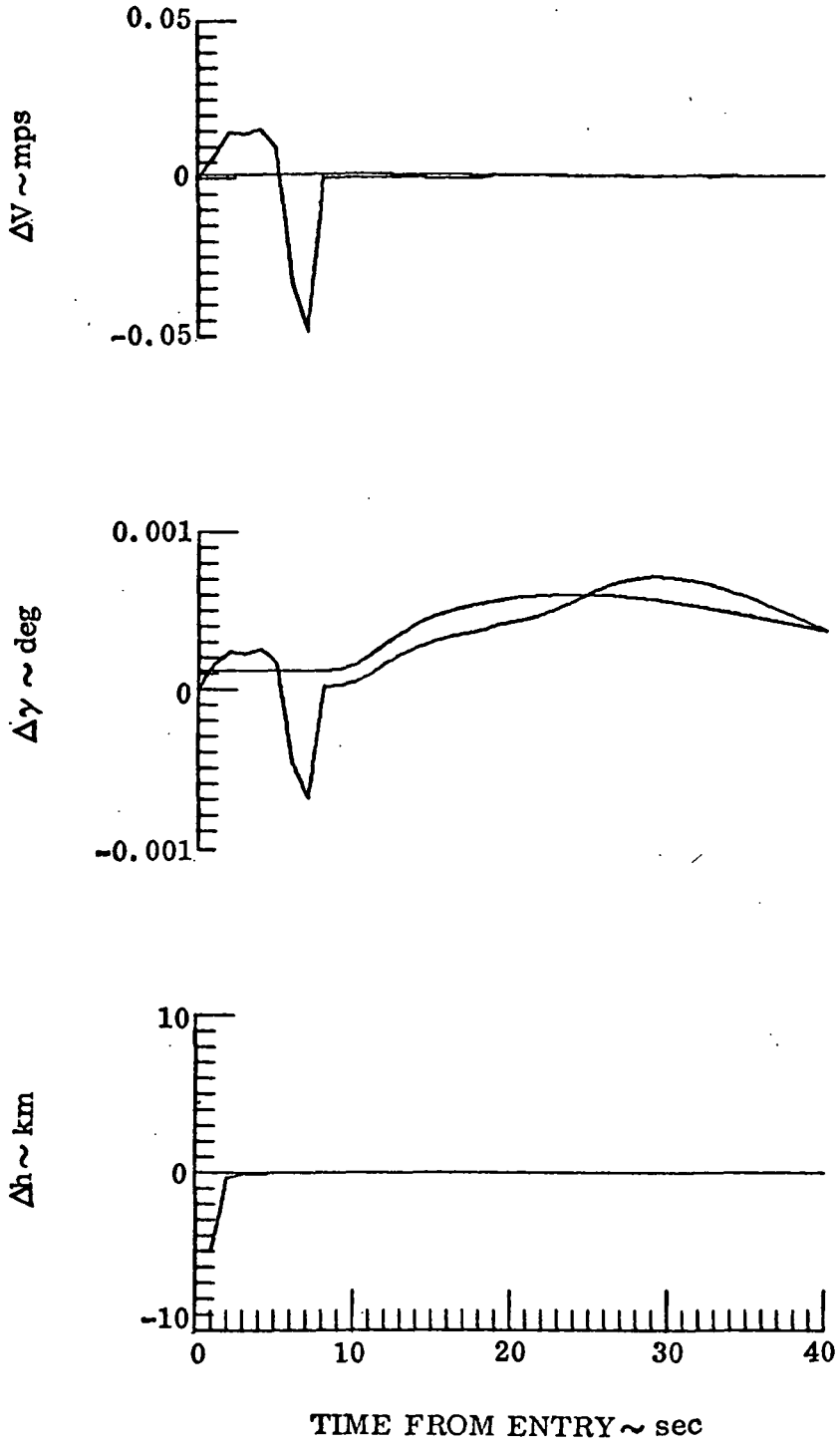

Fig. IV-2 DETERMINISTIC RECONSTRUCTION - INITIAL ALTITUDE ERROR SIMULATED

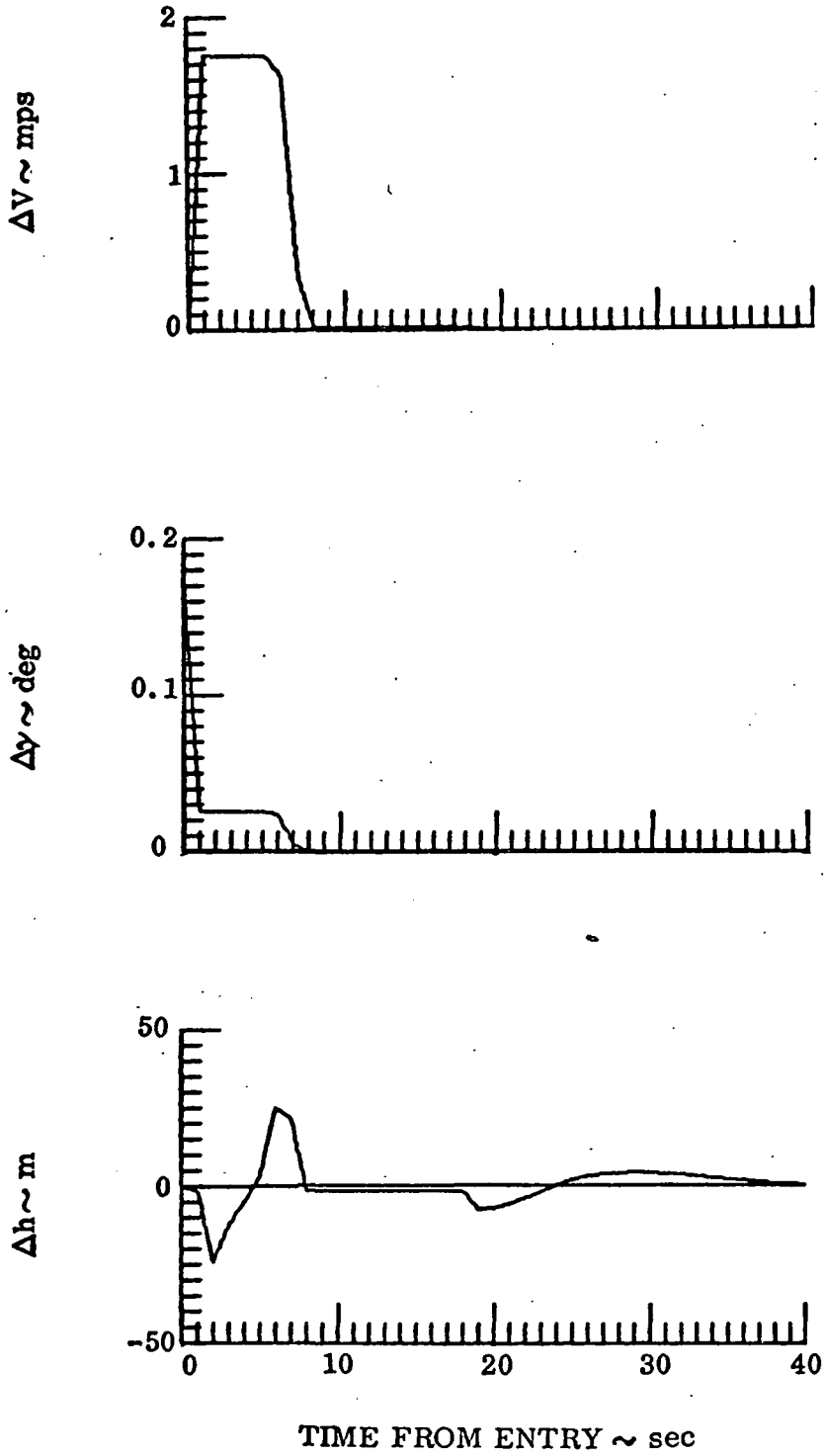

Fig. IV-3 DETERMINISTIC RECONSTRUCTION - INITIAL FLIGHT PATH ANGLE ERROR SIMULATED

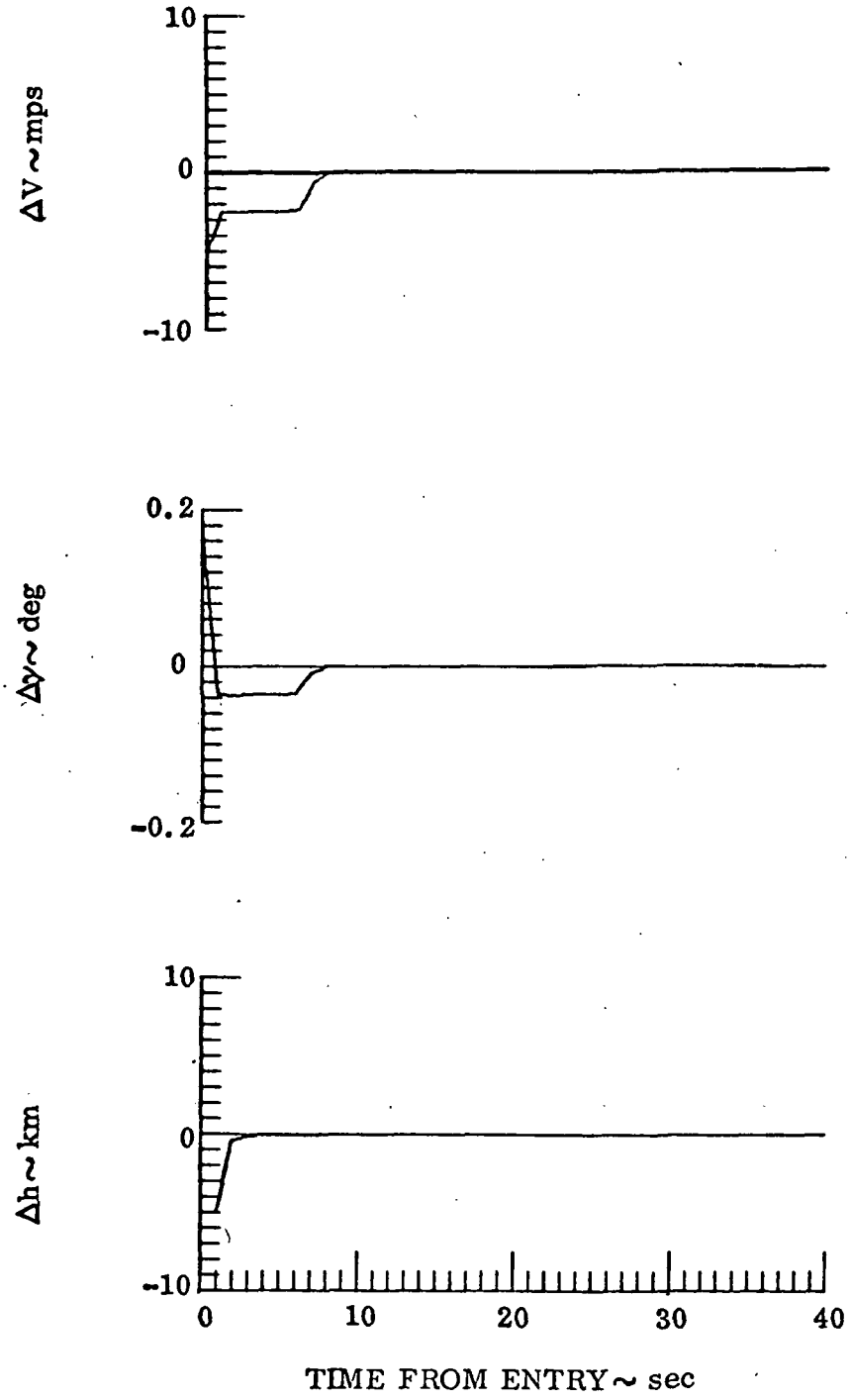

Fig. IV-4 DETERMINISTIC RECONSTRUCTION - COMBINED OFFSET CASE

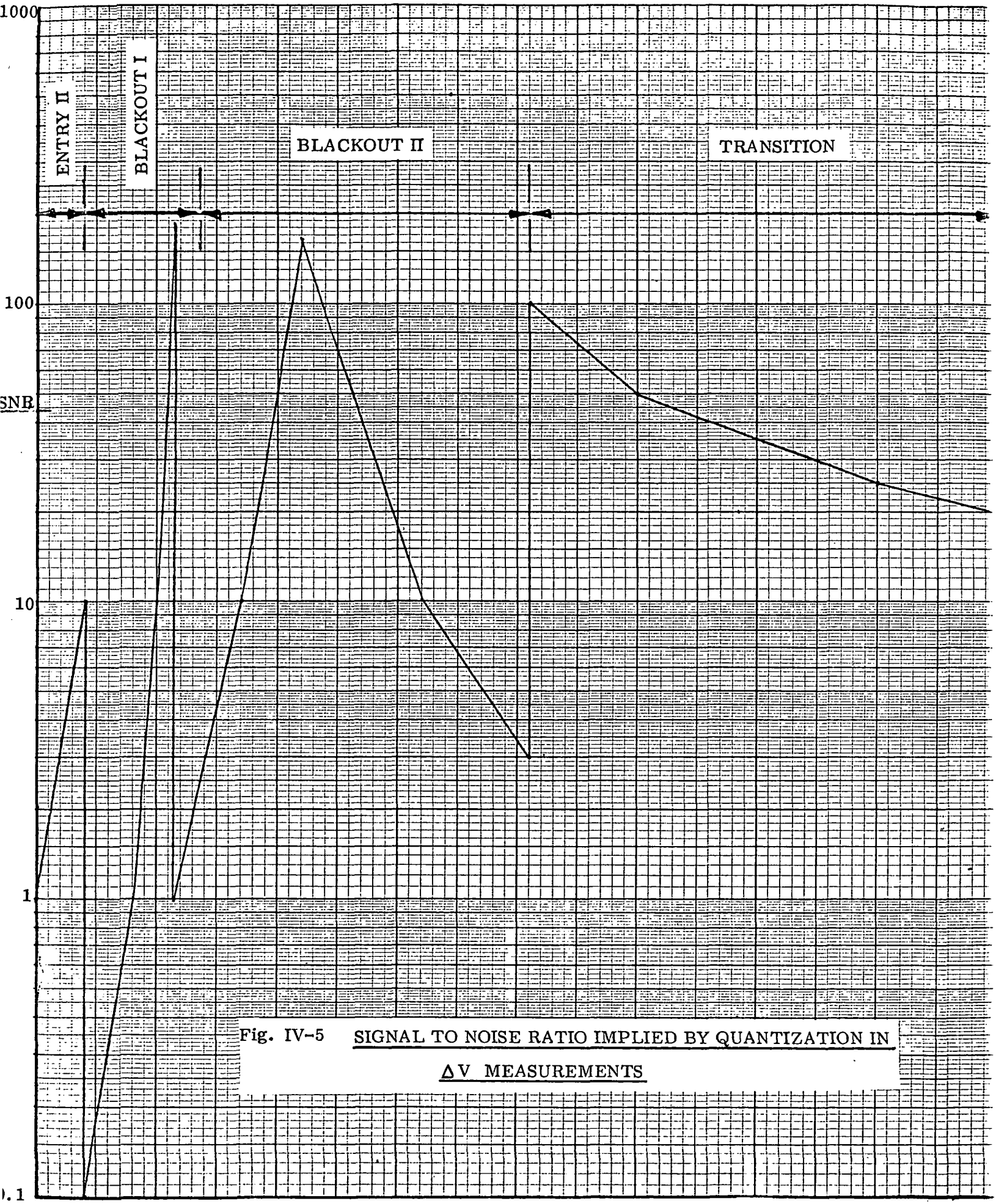

Fig. IV-5 SIGNAL TO NOISE RATIO IMPLIED BY QUANTIZATION IN ΔV MEASUREMENTS

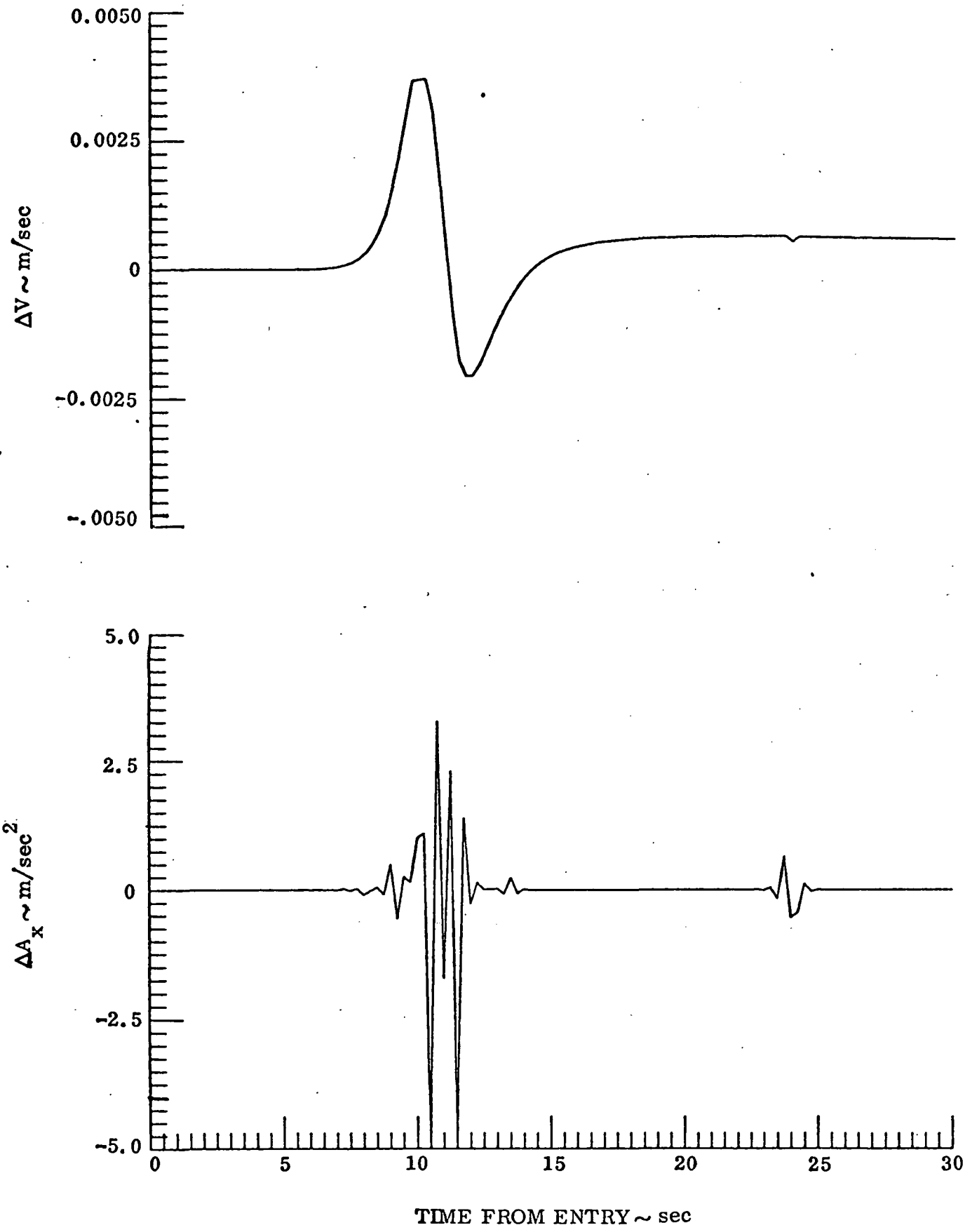

Fig. IV-6 DETERMINISTIC VELOCITY PREDICTION ACCURACY USING CUBIC SPLINE DERIVED ACCELERATIONS

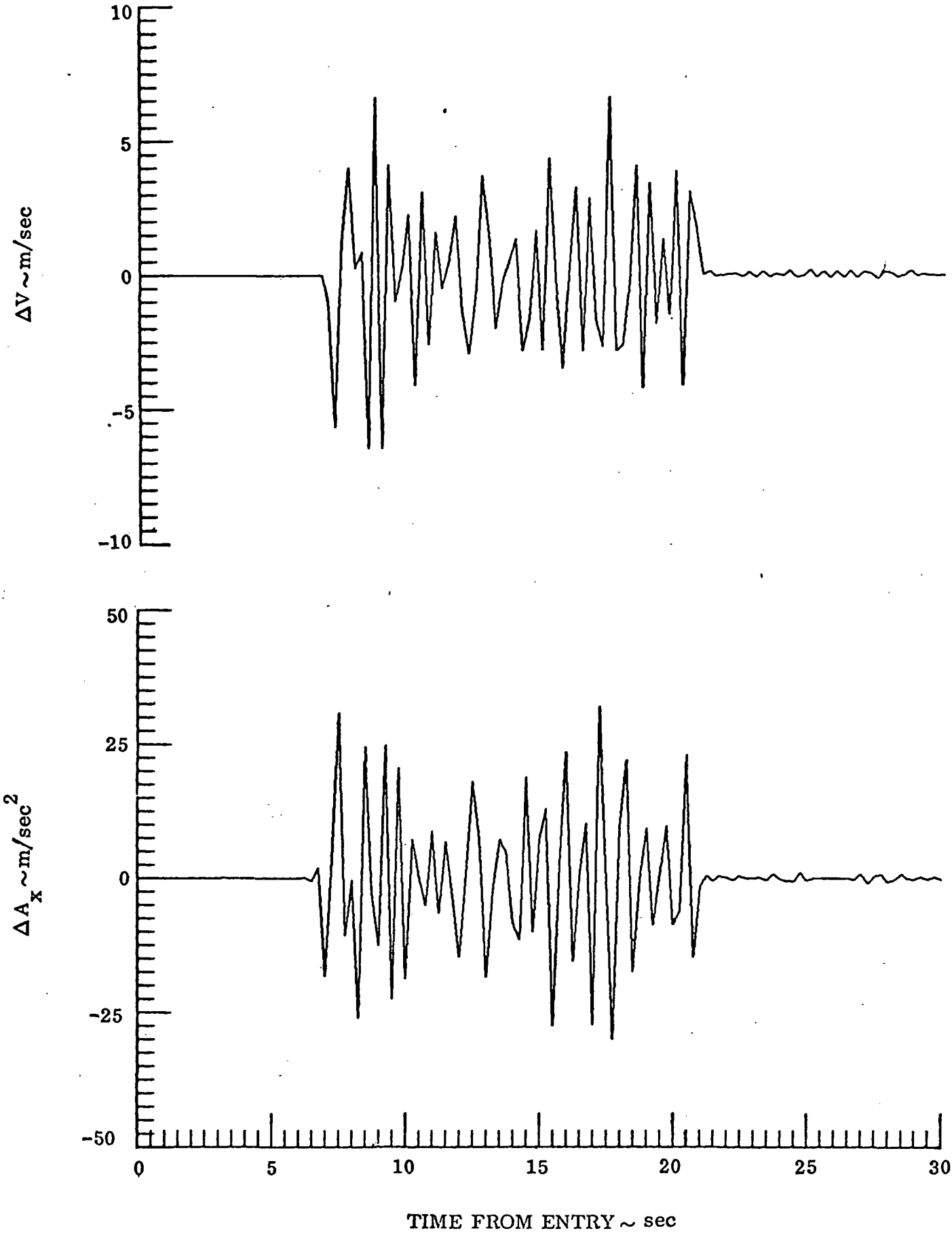

Fig. IV-7 EFFECT OF QUANTIZATION NOISE ON DETERMINISTIC VELOCITY PREDICTION ACCURACY

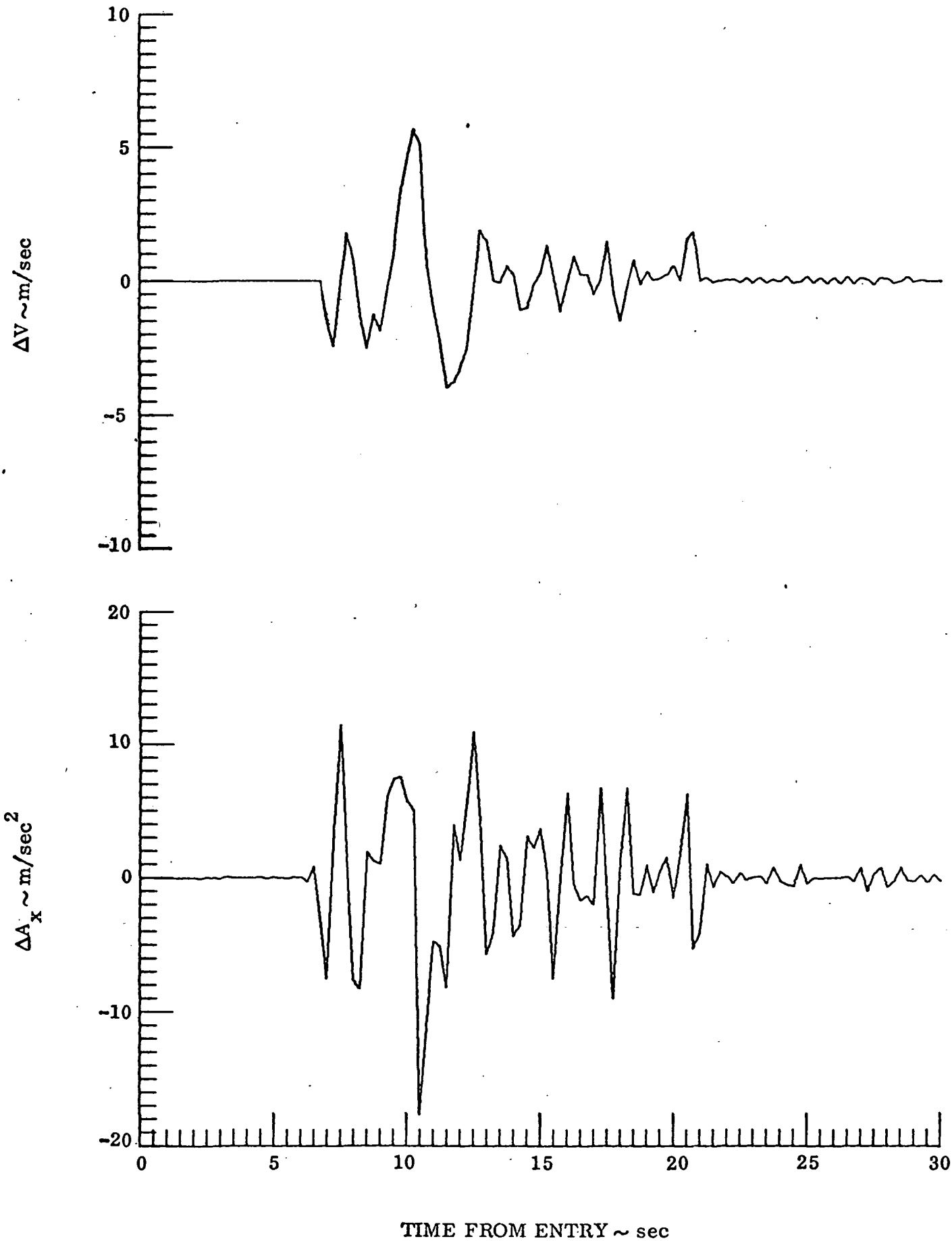

Fig. IV-8 EFFECT OF SMOOTHING ON DETERMINISTIC VELOCITY PREDICTION ACCURACY (S = 10)

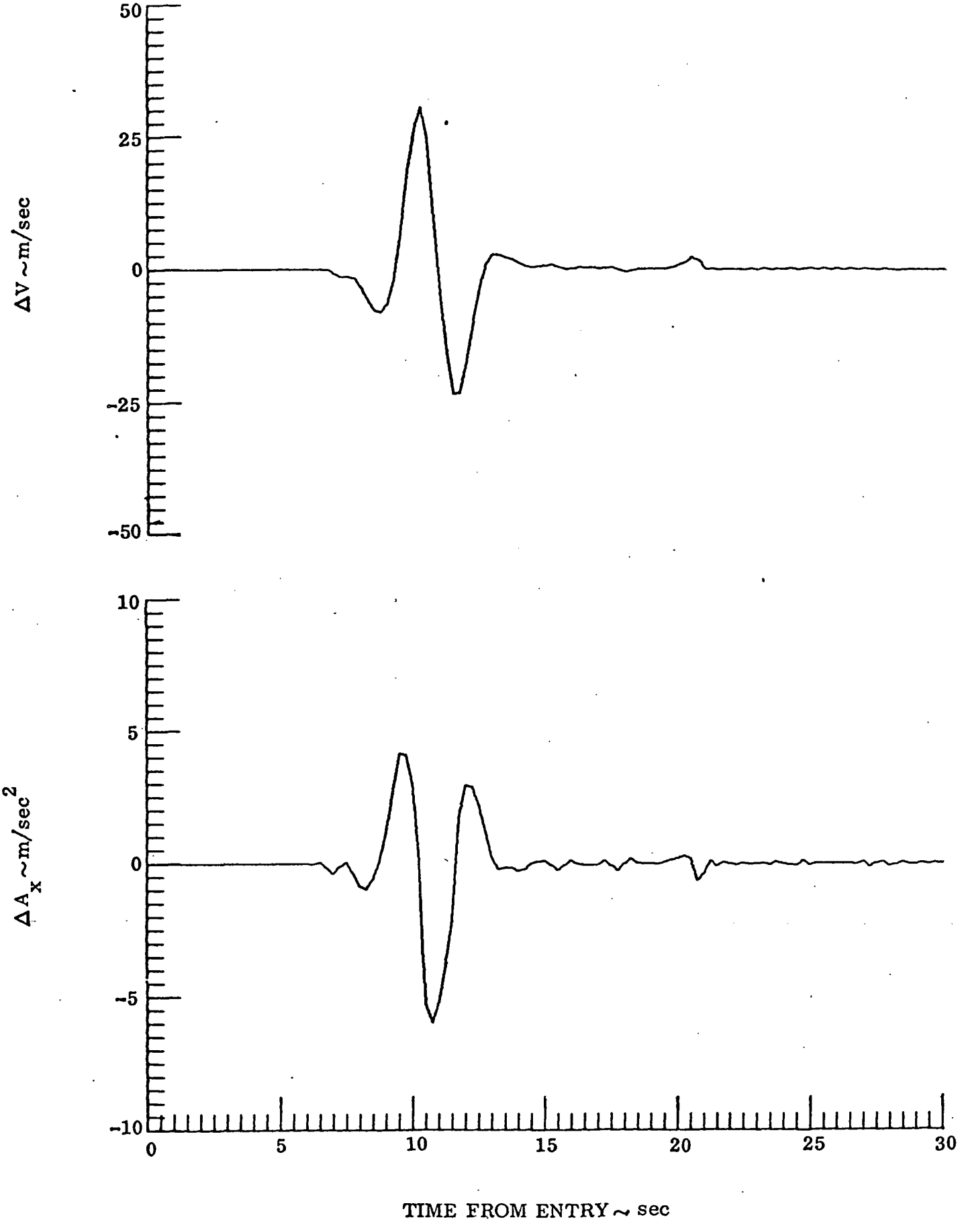

Fig. IV-9 EFFECT OF SMOOTHING ON DETERMINISTIC VELOCITY PREDICTION ACCURACY (S = 100)

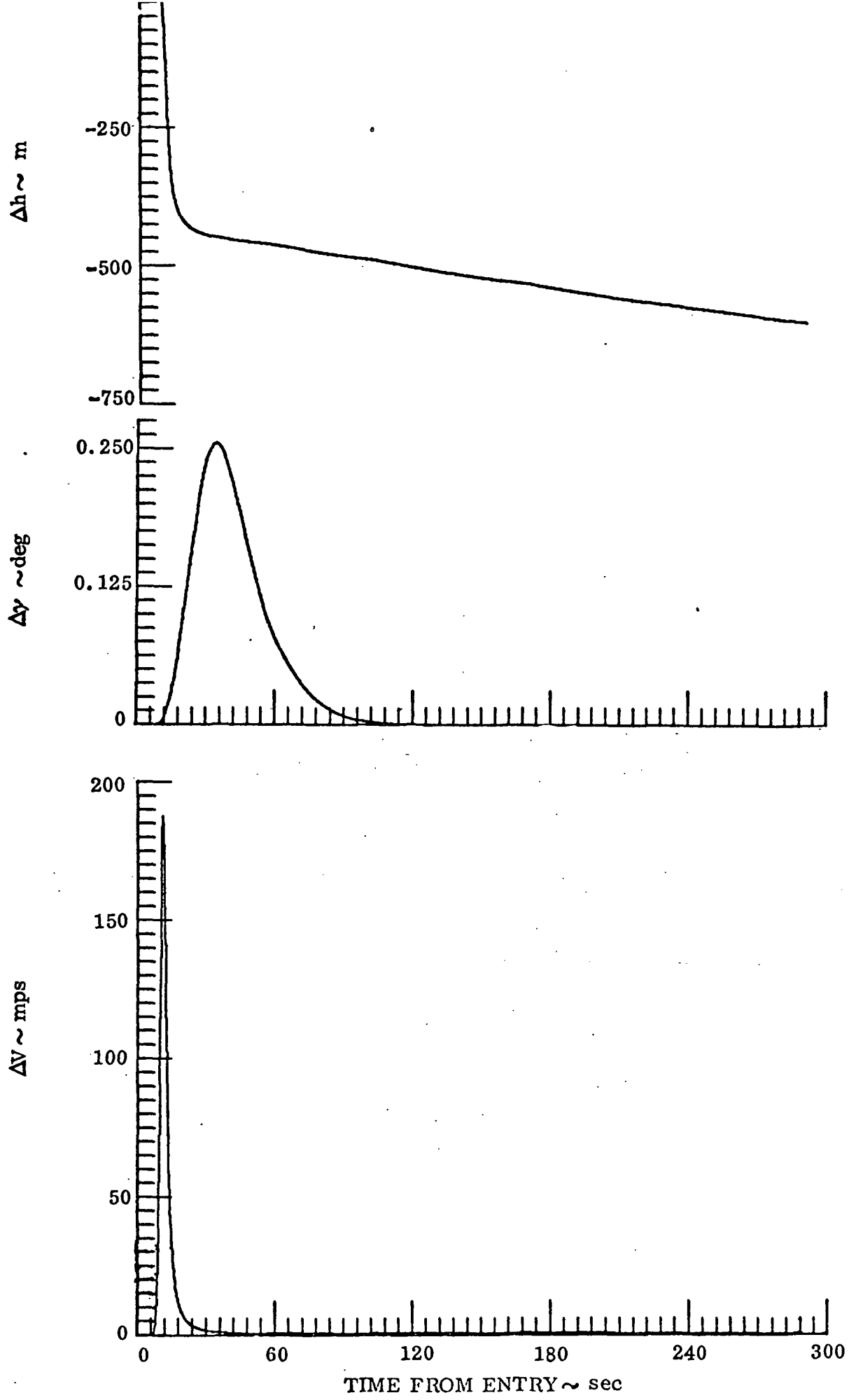

Fig. IV-10 EFFECT OF 10% ρ SCALE FACTOR ERROR ON TRAJECTORY (CONVENTIONAL COWELL INTEGRATION)

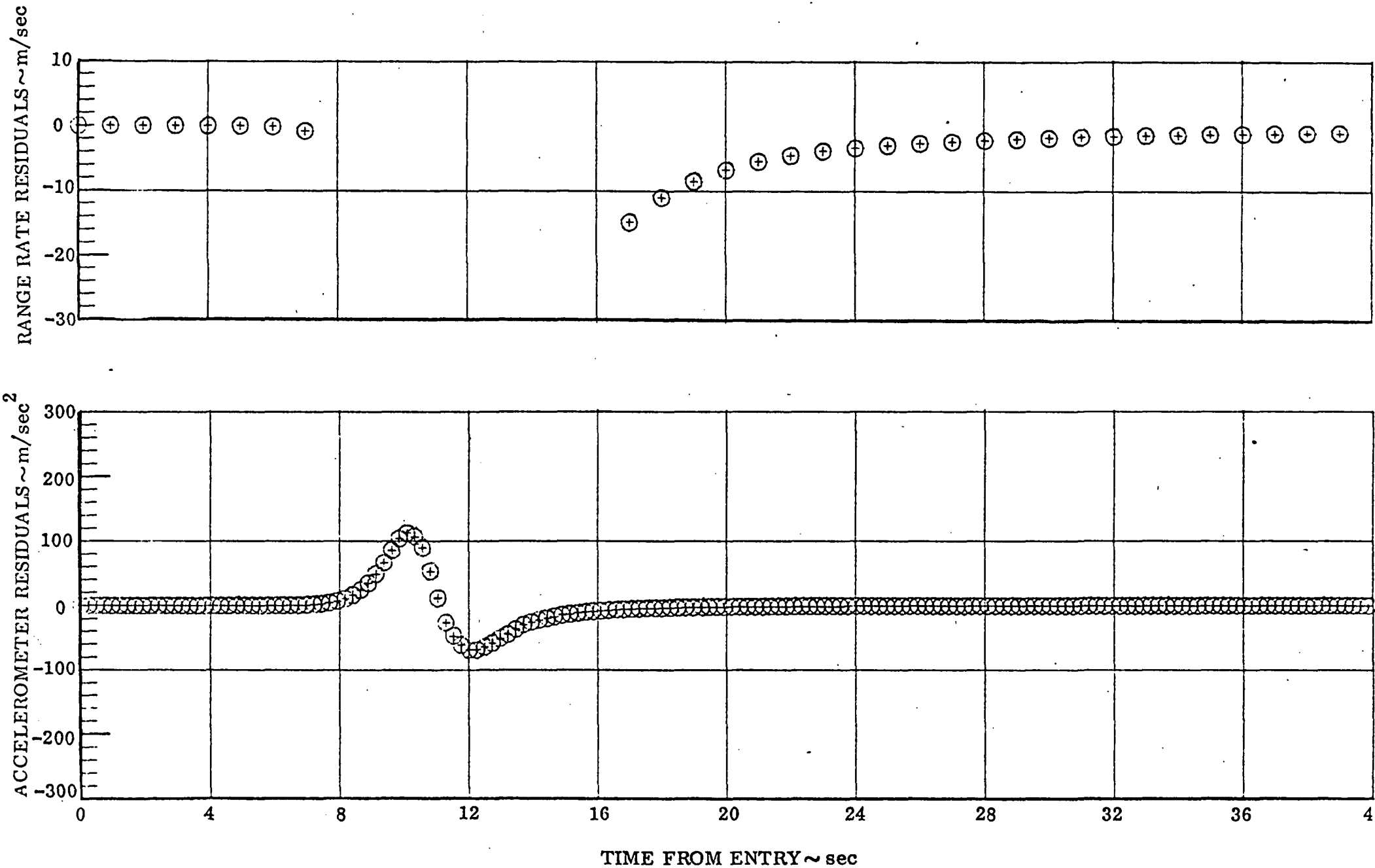

Fig. IV-11 INITIAL RANGE RATE AND ACCELEROMETER RESIDUALS

10% Density Error

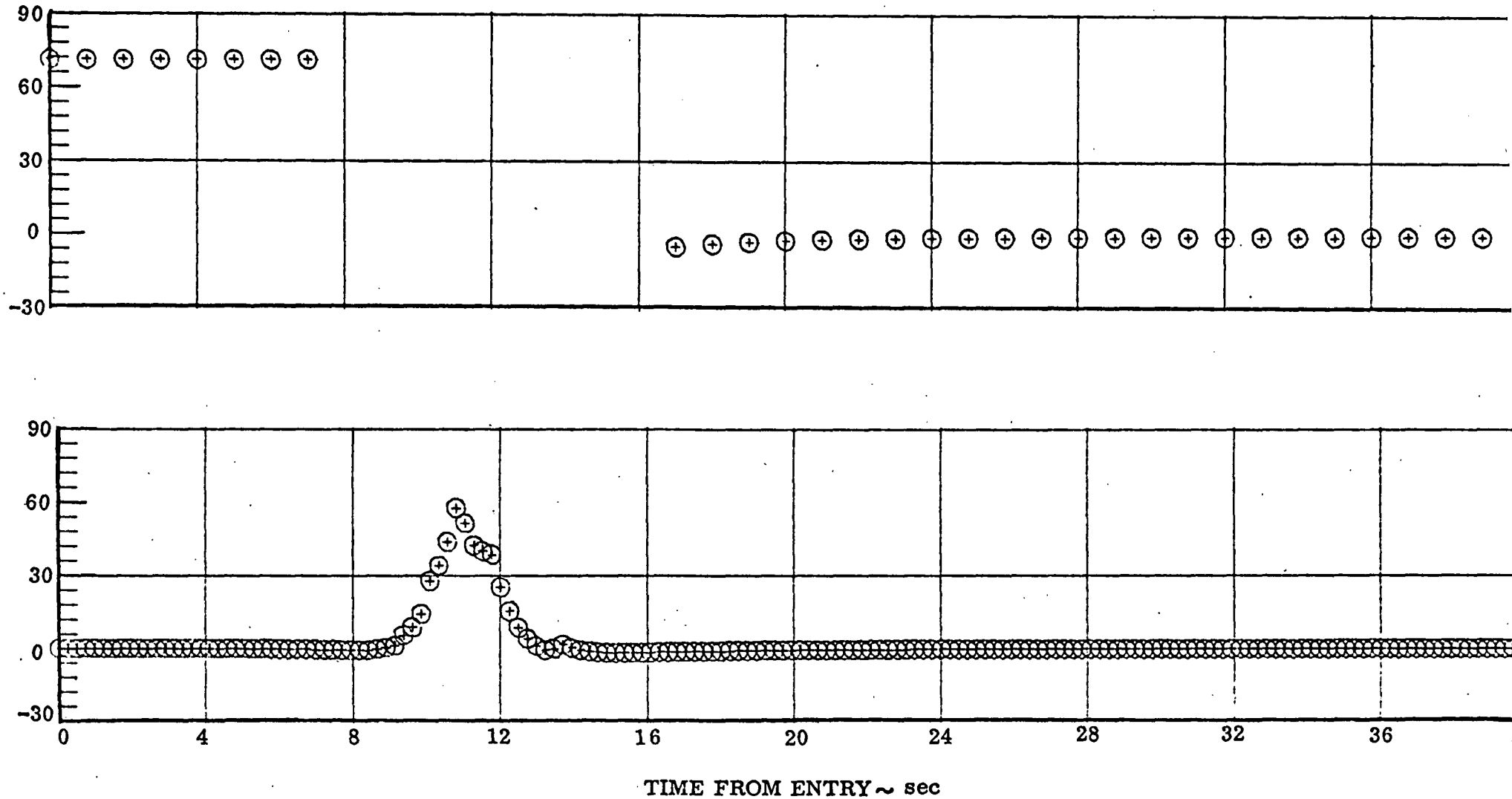

Fig. IV-12 FINAL RANGE RATE AND ACCELEROMETER RESIDUALS (Accelerometry Processing Only)

10% Density Error

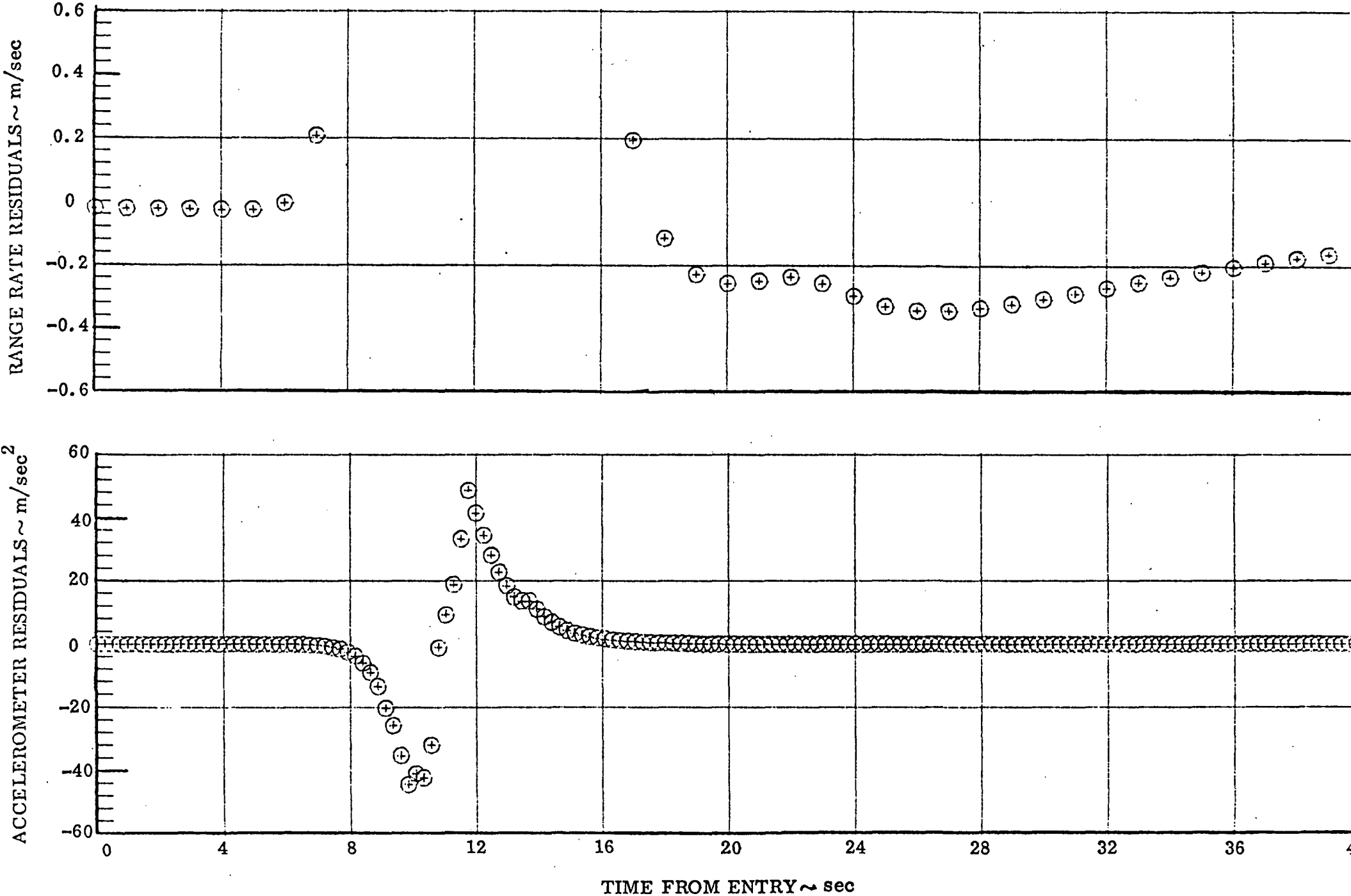

Fig. IV-13 FINAL RANGE RATE AND ACCELEROMETER RESIDUALS (Combined Data Processing)

10% Density Error

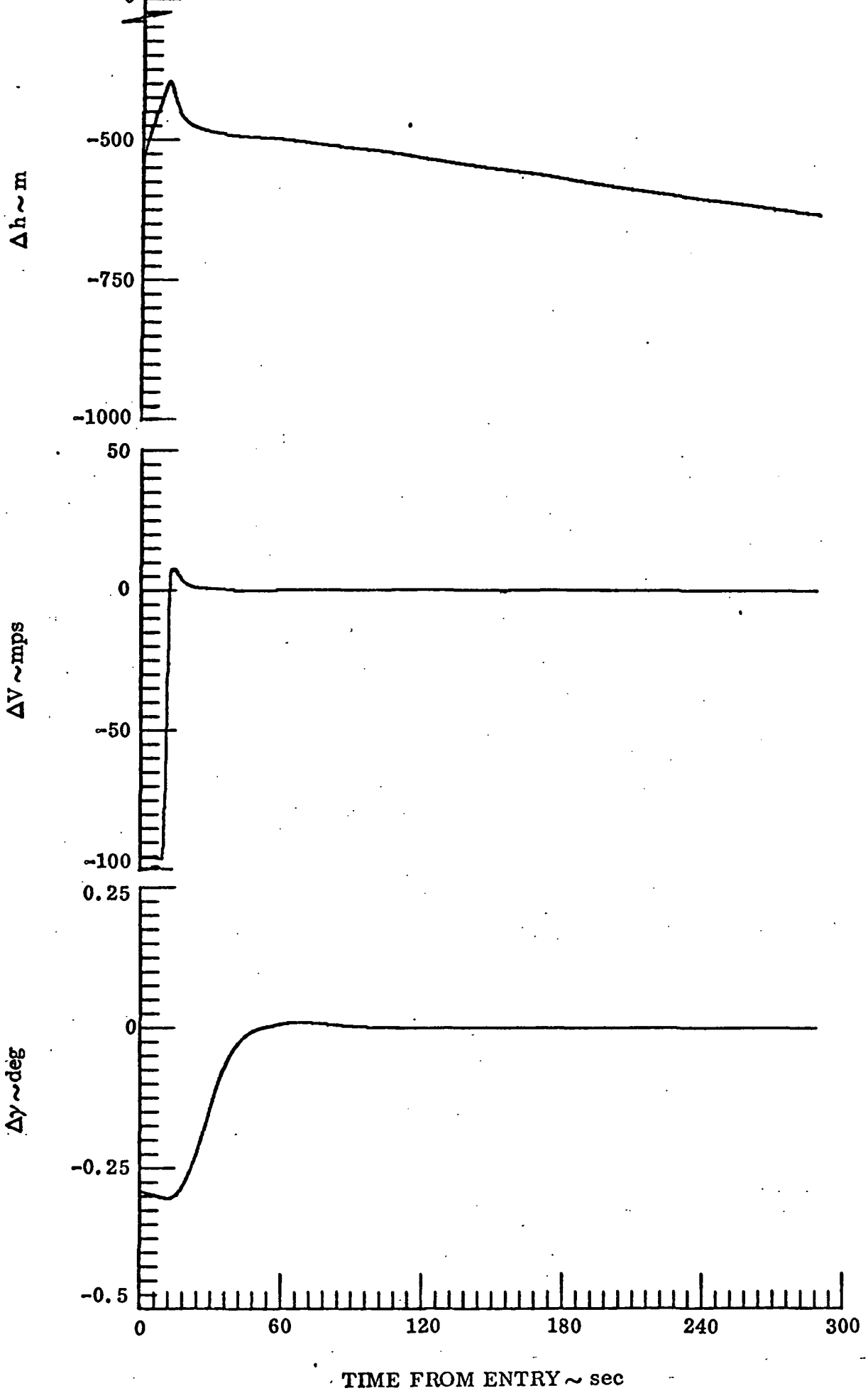

Fig. IV-14 CONVERGED STATE (ACCELEROMETRY ONLY/10% DENSITY ERROR)
(MAPPED VS REFERENCE)

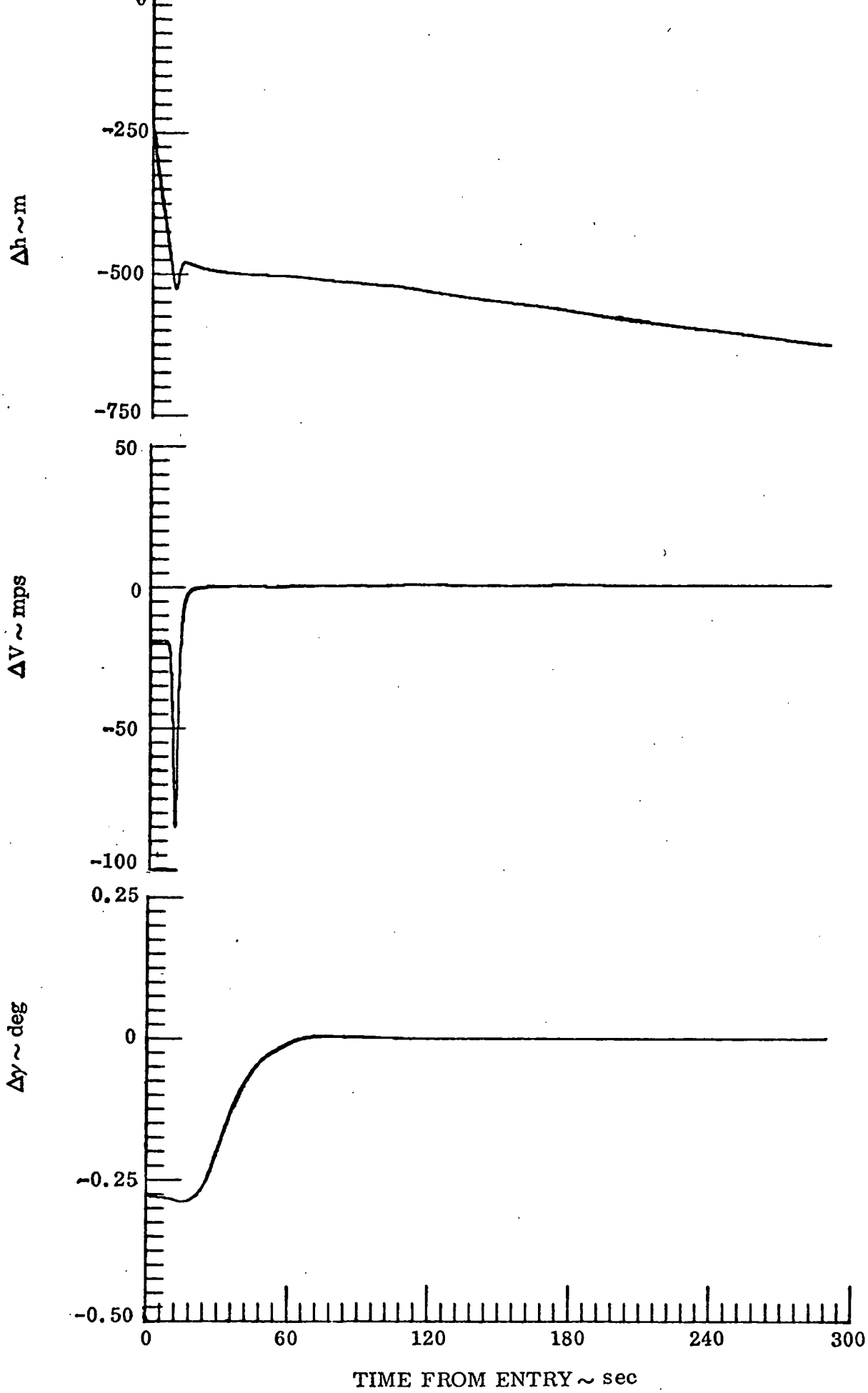

Fig. IV-15 CONVERGED STATE (COMBINED DATA PROCESSING/10% DENSITY ERROR)
(MAPPED VS REFERENCE)

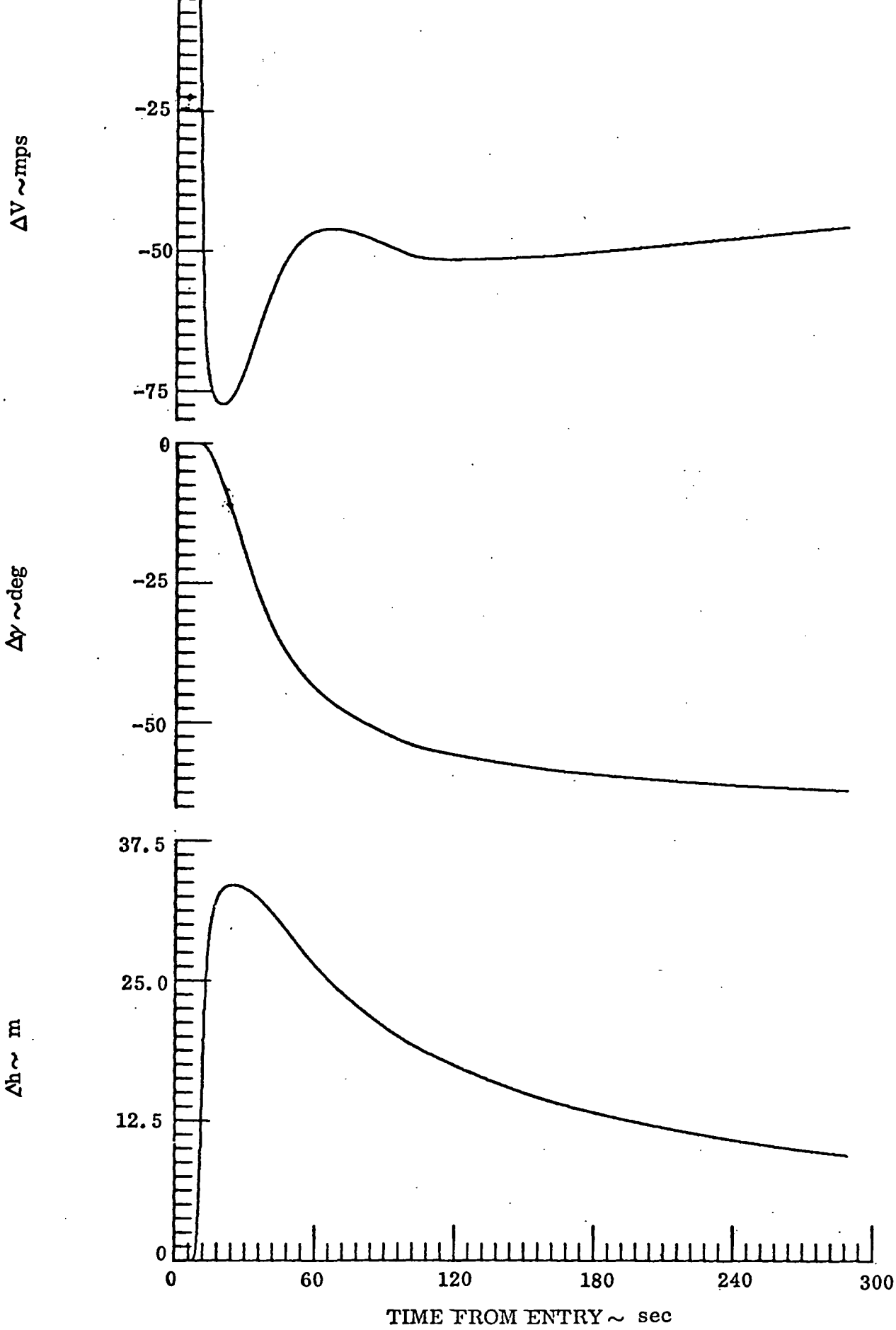

Fig. IV-16 CONVENTIONAL PREDICTION ERROR DUE TO ATMOSPHERIC WIND

(100 mps East Wind)

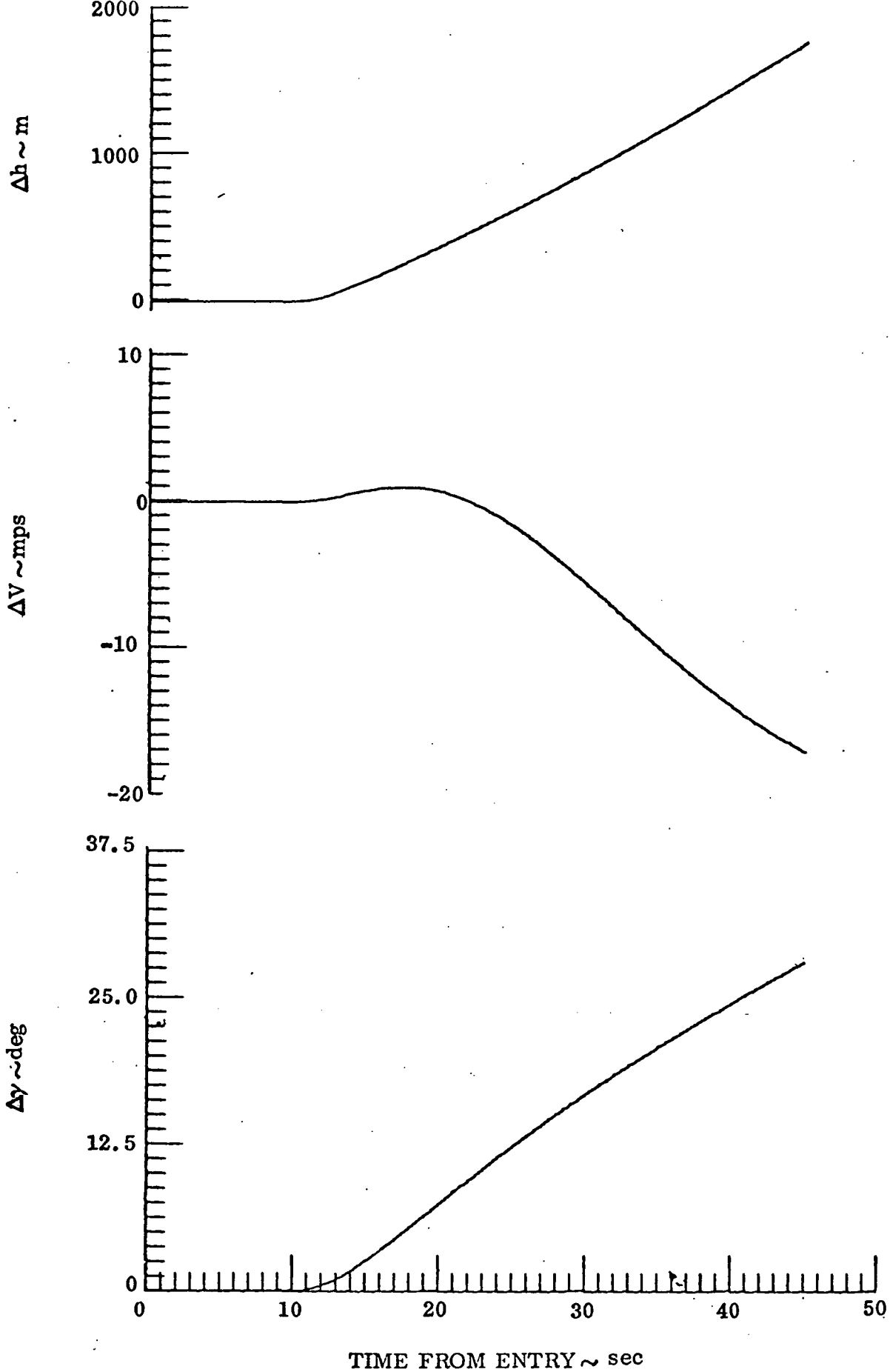

Fig. IV-17 DETERMINISTIC PREDICTION ERRORS DUE TO ATMOSPHERIC WIND

(100 mps East Wind)

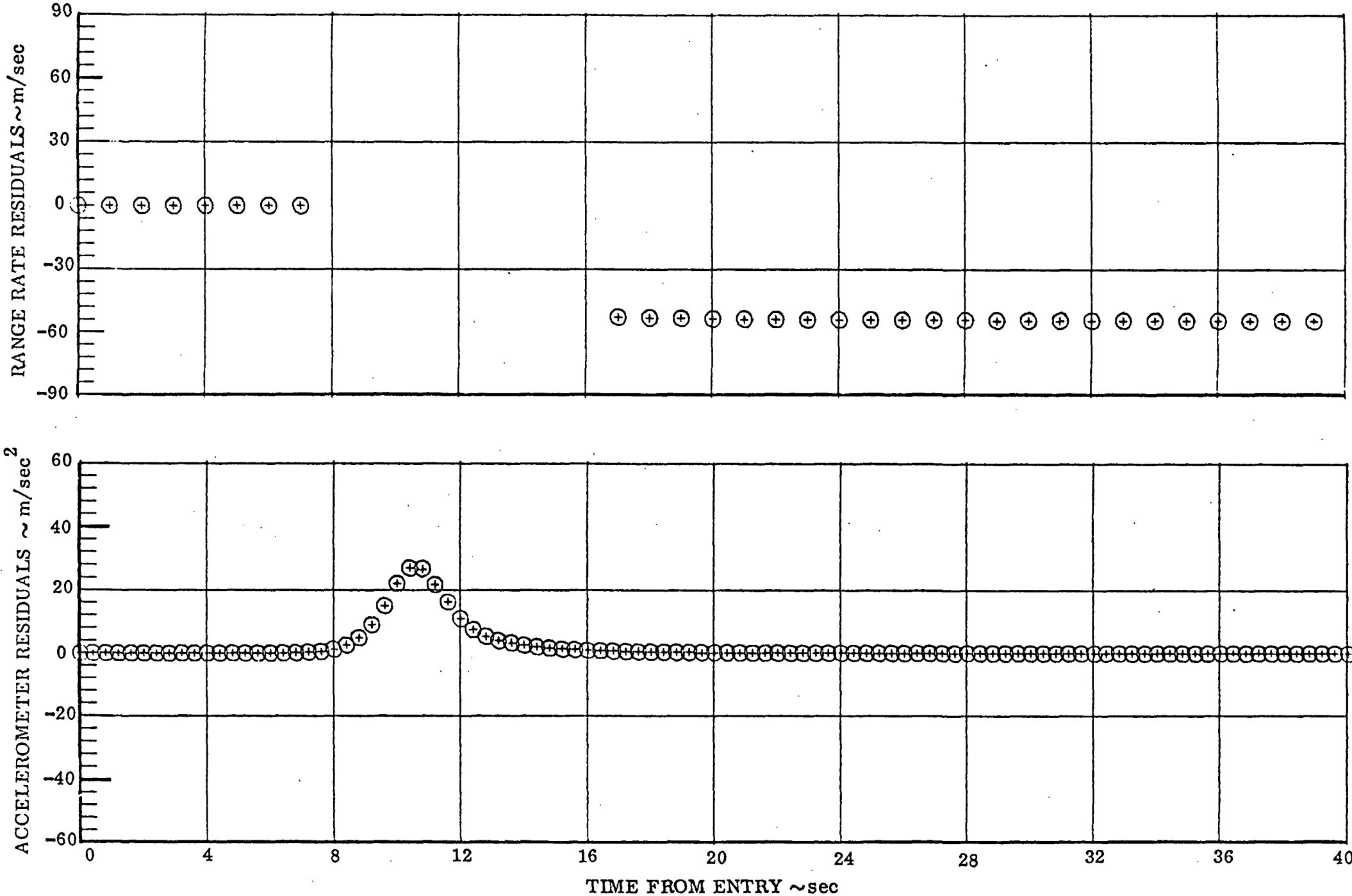

Fig. IV-18 INITIAL RANGE RATE AND ACCELEROMETER RESIDUALS

(100 mps East Wind)

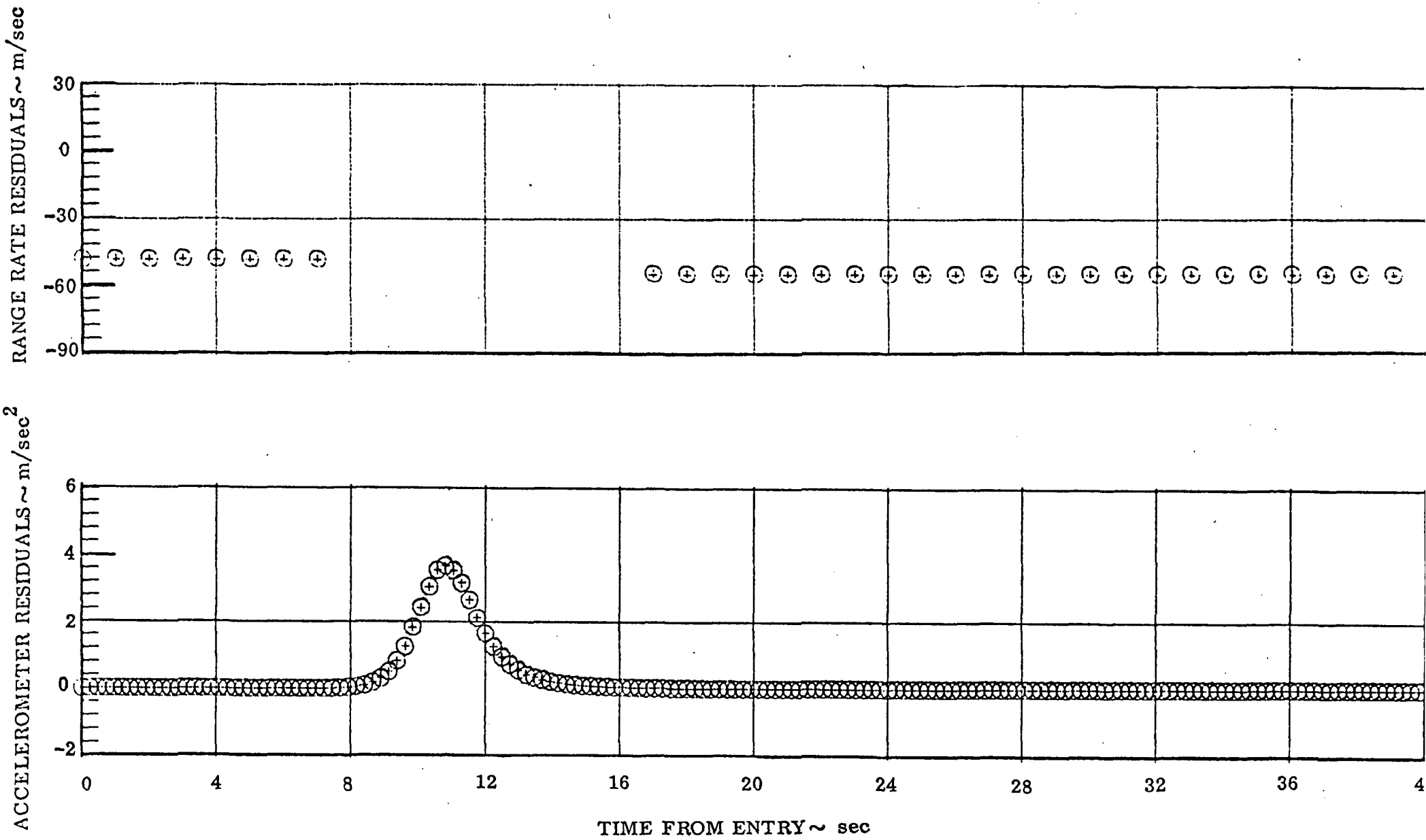

Fig. IV-19 FINAL RANGE RATE AND ACCELEROMETER RESIDUALS (ONLY ACCELEROMETRY PROCESSED)

(100 mps East Wind)

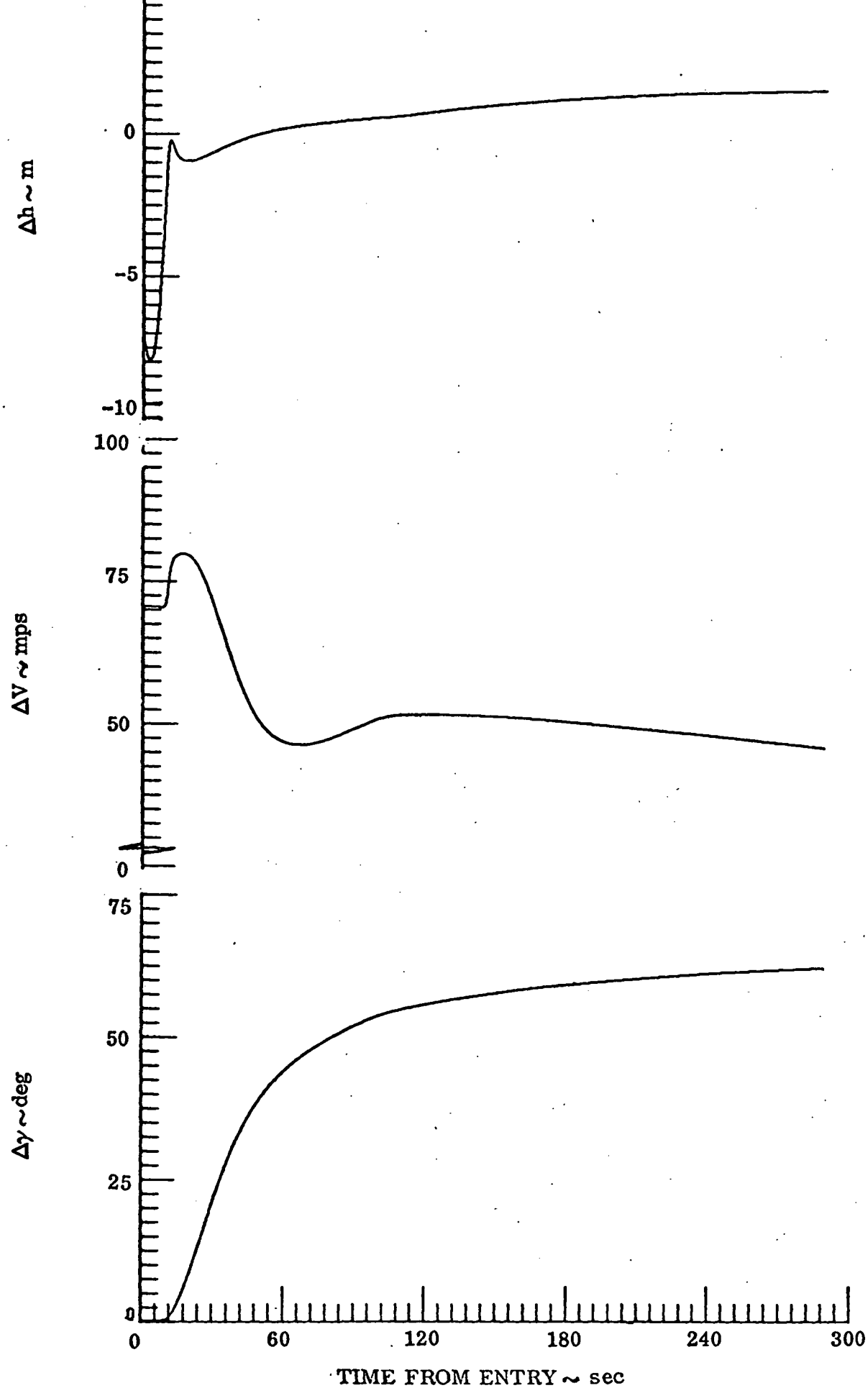

Fig. IV-20 CONVERGED STATE (ACCELEROMETRY ONLY/WIND MODELLING ERROR)

(MAPPED VS REFERENCE)

V. DATA PROCESSING REQUIREMENTS

This section discusses the necessary interfaces that would be required to enable reconstruction of the P/V multi-probe entries. Recommended data processing techniques are also discussed.

V. A. Interfaces

The simplest interface for the radio metric data is the output of the JPL Orbit Data Editor (ODE). These OD files are, in essence, the same files used at LaRC for the Viking experiments. Whereas the DSN/VMCCC at the JPL have revised their data interfaces with the Projects since the Viking era the resultant data transmittal is unaffected. Doppler at 10/sec is recommended during the upper entry segment. One per sec data is deemed more than sufficient during the long vertical coast.

The telemetry interface with Ames is also a straightforward transfer of data. The stations transmit an Intermediate Data Record (IDR) to the Pioneer Mission Operations Control Center (PMOCC). These data are processed by Bendix to create an Experimenter Data Record (EDR). Further decommutation will be done by Informatics under contract to the Atmospheric Structures Experiment Team. Basically this output will be as follows; a calibrated EDR to account for biases, scale factors, etc. (in engineering units) and a limited EDR (calibrated pressure, temperature, and acceleration data with time). Experimenters at LaRC most probably need be concerned with the limited EDR only.

Care must be exercised to sync the station time, spacecraft time properly since Earth based Doppler data are observables to be processed in concert with accelerometer data tied to a spacecraft clock. This was not nearly as significant for Viking since no remote observables were processed. The Viking spacecraft was completely autonomous in this sense, all events and measurements were handled from the common baseline of GCSC time from spacecraft separation.

Supplementary Experimenter Data Records (SEDR's) necessary are the converged solutions obtained by the JPL navigation team. States and covariance

information at the entry interface are required. A copy of the JPL OD Lock Files, which prescribe all the necessary input parameters, is also needed. In addition the particular Development Ephemeris used for the P/V mission must be adopted.

V.B. Telemetry Data

A cubic spline differentiation process is recommended to reduce the measured ΔV's to the acceleration level. The differentiation routine, SPLDER , is available on the LaRC program library FTNMLIB. A theoretical discussion of the technique is given in Ref. 9. The program performs a cubic spline approximation, differentiation and interpolation on an input functional. The first and second derivatives are continuous although the jerk term is not differentiable. It was shown that with perfect ΔV data the spline derivative routine can extract acceleration information data reflecting finer structure in the curve than is otherwise available at the 0.25 sec spacing.

Considerable time was spent applying this technique to the Viking X-channel ΔV measurements and the results look promising. The routine does, however, track the quantization noise since it operates between consecutive points on the input file. For Viking the level of the maximum acceleration is down by a factor of 50 or so and the duration of the peak g pulse is much longer in time. It was shown that some inherent smoothing could be obtained for Viking data by not applying the spline derivative routine to each point. Viking enjoyed the privilege of ample data return. Data for Viking were transmitted at 0.1 sec intervals. Accelerations were generated using every 5th, 10th and 50th point on the total accumulated velocity file. Even for every 50th point (equivalently a 5 sec data rate for Viking) the reconstructed acceleration time history look reasonable. The Pioneer Venus entries are far more dynamically interesting near peak g and the 0.25 spacing is felt to be marginal at best. However during intervals on either side one could obtain smoothing by spline differentiating every nth point.

There is another smoothing concept which has been identified. There exists a cubic spline smoothing routine, CSDS, on the LaRC library. This routine was used to smooth a simulated quantized ΔV file for the Pioneer entry. Results are presented earlier in this report in Section IV. C.4. The routine computes a cubic spline, G (x) , from an input file (x_i , F_i) having the following properties:

$$(1) \qquad \sum_{i=1}^{n} \left(\left(G(x_i) - F_i \right) / W_{F_i} \right)^2 \leq S$$

and (2) $\int_{x_1}^{x_n} \left[G''(x) \right]^2 dx =$ minimum of all splines satisfying (1) above

The W_{F_i} are weights which are input to reflect the varying levels of quantization contained on the input file.

The smoothing parameter, S , controls the degree of smoothing ($S \equiv 0$ specifies no smoothing at all). As shown previously smoothing increases the local error near the dynamic peak g region.

It has not been expressly shown that the accelerometry, used as external observables in the conventional scheme, need be smoothed at all. The proper data weighting scheme, one which reflects the variable quantization noise with time, can prevent the filter from chasing noise. This does tend to downweight the data as discussed previously in this report.

V. C. Tracking Data

As mentioned earlier the OD Files transmitted from the JPL are the usual interface with the LaRC experimenters. It is recommended the OD Files be created at a 10 per sec rate during the upper entry segment. A one per second compression during the vertical phase is more than sufficient.

It must be recognized that the 1-way Doppler observable represents a unique data type for navigation. Section VII and Appendix A delinates some concerns felt to be rather important for this observable. Some corrections to both

the 1 and 2-way Doppler data to account for the Venus atmospheric effects will most probably be necessary, particularly at the lower altitudes. This should be coordinated with either the JPL or the DLBI investigators at MIT, Dr. Councilman, et al.

VI. RECOMMENDATIONS (TASK III)

In the absence of gyro data (and probable existence of winds) it was concluded that the Viking deterministic concept was not suitable for the Pioneer Venus multi-probe reconstruction. Perhaps some use of this concept to provide for a first-order density update is feasible but this must be planned for adaptively. It certainly could be attempted and interpretation of the results may imply the existence of winds given that the atmospheres in Ref. 4 represent a reasonable bound. Another indicator of existing atmospheric winds will be the Doppler residuals. However, any indications of upper altitude winds will compromise the resultant density determined from this simple pseudo altimetric shifting scheme and thus negate using the derived density profile.

For the Pioneer Venus multi-probe mission the conventional batch orbit determination procedure is recommended. Eventhough the spacecraft predictions are subject to modelling errors the filtering algorithm does not absorb these modelling deficiencies in the state estimate. There is no state variable, or any other model parameter for that matter, that yields a Doppler signature which can, in any way, be correlated with that induced by atmospheric winds. For a simple density modelling error (constant scale factor multiplier) the effects are also unique. State solutions in the presence of this type scaling error on density do not provide a good fit to the data. It must be understood that density is highly correlated with the spacecraft ballistic parameters.

It is felt that these atmospheric parameters can be solved for. Therefore, it is recommended that they be formally added as solution parameters. Physically motivated models should be adopted. The solution set will obviously increase. A concept of altitude layering must be adopted. In each layer density scale height, wind velocity and perhaps gradients, and wind direction (as examples) must be determined. It should be pointed out that in some layers, in particular when determining density, the model parameters and state parameters may be more strongly correlated. However, in the large it is felt that initial state errors can be uncoupled. This concept must be simulated and a series of test cases made to quantify the results.

VII. CONCERNS

The principal concern as to the adequacy of the recommended process, or for that matter any process, has to be the 1-way Doppler. This data type has not been used as a principal navigation data source and must be considered a relative unknown. The ongoing Voyager spacecraft has an ultra stable oscillator (USO) with a specification on stability on the order of 4 parts in 10^{12}. A pass of 1-way data on Voyager showing residuals for the 1-way data compared against computed values (based on an accurate 2-way solution) would indicate a short term stability on the order of 10^{-14}. The Pioneer Venus spec value of 1 part in 10^9 can possibly result in noise on the order of 2 Hz (several tenths of a mps) if the actual stability is achieved. It is obvious this noise either increases or decreases dependent upon the actual stability of the oscillator. An added concern re the 1-way data is the warm-up characteristics. One must remember the spacecraft is only powered-up 20 min prior to entry so the oscillator must achieve its stable frequency quickly. The first indication of any 1-way problems will most probably occur during the JPL processing to refine the spacecraft estimates at the entry interface.

An additional concern is the effect of the Venusian atmosphere on the radio signal during entry. Both 1-way and 2-way Doppler are affected. Some model of the neutral atmosphere effects will most probably be required. There will be no data available for charged particle calibrations.

The quantization error on the accelerometry represents a modest concern for the recommended procedure. Over much of the interval during BLACKOUT II the signal to noise is quite small. Properly weighted, of course, this is not catastropic. However, it does tend to reduce some of the information content in these observables. Having less accurate accelerometry is really important if the Doppler data is rendered useless because of any unforseen occurrence. However, there are instantaneous acceleration measurements, which are less frequent but much more accurate, which will help alleviate any problems.

It has been shown that the process separates model and state parameters, i.e., the filter cannot make state corrections to absorb the modelling errors and achieve a good fit to the data. It has been recommended herein that physically

motivated models be included in the process as solution parameters. This will necessarily increase the number of solve fors. Until simulated and analyzed one cannot quantitatively define the accuracy with which atmospheric model parameters can be estimated.

VIII. SUMMARY

Two methods, the Viking deterministic concept and a conventional orbit determination method, have been evaluated for applicability in the reconstruction of the Pioneer/Venus multi-probe trajectories. The latter method has been recommended. The deterministic method offers some advantages but, due to the lack of gyros, restrictive assumptions as to spacecraft attitude must be made. These assumptions in essence reduce the Viking concept to a point mass program. For the most part this limitation is quite adequate. However, the presence of atmospheric winds, a very probable situation, inviolates the assumptions necessary to make the Viking concept workable. Without gyros the necessary information to determine the winds is lost. It is shown that the conventional batch processor is very dependent on a priori modelling of the spacecraft and atmospheric parameters. There is, however, strong indication that the model parameters may be determinable by combined data processing using both the Doppler and accelerometry. It is recommended herein that the appropriate program modifications be made to formally add this capability in the solution set.

Data pre-processing requirements are delineated herein. A cubic spline derivative routine is recommended to reduce the accumulated ΔV measurements to the equivalent acceleration level. A cubic spline smoother was shown to be effective in smoothing the data prior to differentiation. The requirement to do this is not patently obvious.

Some concerns are indicated which can impact the overall accuracy of the reconstruction process. These can simply be summarized as:

(1) quantization level on the ΔV measurements;

(2) potential 1-way Doppler problems;

and (3) the influence of the Venusian atmosphere on the radio signals.

APPENDIX A

MEASUREMENT NOISE MODELS

Doppler Data

The usual method of describing Doppler noise is based on the truncation within the Doppler counter per se since the frequency standards at the DSN stations are extremely stable. The Doppler counter accumulates zero crossings within a given interval. It is possible to be off by one count over said interval. Thus, for a one minute count time the noise model is 1/60 or 0.015 Hz. This is equivalent to ~ 1 mm/sec for 2-way data and ~ 2 mm/sec for 1-way data. Since the truncation error is dependent upon the count interval the following adjustment is made:

$$\sigma_c = \bar{\sigma} \sqrt{\frac{60}{t_c}}$$

where $\bar{\sigma}$ is the noise for a 1 minute count time

and, σ_c is the adjusted noise for the actual count time, t_c (sec).

This noise model is very conservative for 2-way data. It is felt that this model is optimistic for 1-way data.

An alternate noise model for the 1-way Doppler, based on the oscillator instability (1 part in 10^9) for the small probes, is perhaps more realistic for Pioneer Venus. At S-band this instability amounts to a 2 Hz uncertainty, or approximately 300 mm/sec. This model is assumed herein as being independent of count time.

Both 1-way noise models were adopted for the analysis presented in the report.

Accelerometry Data

The P/V multi-probes will make two distinctly different acceleration measurements during entry. The predominant information will be the sensed velocity change undergone at a fixed interval. These measurements are ΔV pulses at

a fixed frequency of 4 per second, at least during blackout.[1] Instantaneous digital accelerations are also read out at 1 per 2 seconds. Scale factor accuracy and short term bias uncertainties for the sensors and associated electronics are sufficiently small. The noise model for the accelerometers is dominated by the quantization error, particularly for the ΔV measurements.

In order to accurately cover the large range of accelerations the probes will encounter the spacecraft, via g-sensing, switch to various modes. These modes and the corresponding quantum accuracies are as follows:

TABLE A-1 ΔV QUANTIZATION LEVELS

MISSION PHASE	SUGGESTED RANGES(g's)	PULSE SIZE (ΔV)
ENTRY I	4×10^{-7} to 10^{-4}	0.0012 mm/sec
ENTRY II	8×10^{-5} to 10^{-2}	0.12 mm/sec
BLACKOUT I	8×10^{-3} to 1.5	1.8 cm/sec
BLACKOUT II	1 to 600	7.2 m/sec
*TRANSITION		18 cm/sec
DESCENT	0 to 1.5	1.8 cm/sec

*The spacecraft switches to the TRANSITION range at 5.5 g's on the downward leg of the pulse and remains for a fixed time interval (32 sec for the large probe, 64 sec for the small probe) defined by 16 and 8 minor frames for the large and small probes, respectively.

Clearly during BLACKOUT II quantization can be significant. The sensor electronics are so designed that no pulses are counted twice, or lost, during interrogation. Therefore, the quantization can vary $\pm$ 7.2 m/sec relative to the actual accumulated counts. At a data spacing of 4/sec this yields, to first order, noise of approximately 56 m/sec^2, peak to peak.

Equivalent random noise levels representative of these quantum levels were adopted for the entry analysis in the report. These equivalent noises(Table A-2) were applied at the acceleration level and are felt to represent a conservative measurement model.

(1) The complete instrument sampling schedule for the probes varies dependent upon the particular Mode.

TABLE A-2

EQUIVALENT RANDOM NOISE TO EMULATE ΔV QUANTIZATION NOISE

MODE	TIME INTERVAL (sec)	σA_x (m/sec^2)
ENTRY II	$0 \; t \leq 2$	0.32 E-3
BLACKOUT I	$2 < t \leq 6.75$	0.048
BLACKOUT II	$6.75 < t \leq 20.5$	19.2
TRANSITION	$20.5 < t \leq 40$	0.48

Another noise model, based on the expected quantization of the instantaneous acceleration measurements, was also used in the analysis. These data, processed at 1 per 2 seconds, were considered accurate to 0.1 m/sec^2.

APPENDIX B

BATCH ORBIT DETERMINATION SOFTWARE

I. Baseline Software

The orbit determination program referred to as the Viking Radio Science Software (VRSS) has been used principally for estimation of Martian gravity field coefficients utilizing the 2-way Doppler tracking data received from the Viking orbiters. A batch, weighted least squares filter is used for parameter estimation. The solution parameters include S/C initial conditions; gravity field coefficients; tracking station locations; heliocentric orbital elements of both the S/C central body and the Earth-Moon Barycenter. In addition, S/C trajectory perturbations due to atmospheric drag (with solution capability for a ballistic coefficient $C_D' = C_D A/2W$) are modelled, but this logic was never exercised for Viking since the orbiters are essentially drag-free satellites.

VRSS is composed of three main elements, which are separate programs interacting via files. The acronyms for each element and the function each performs are as follows:

POWSER	Integration of S/C equations of motion and variational equations using power series methods
NORM	Computes observation (Doppler or range) residuals and regression partial derivatives. Forms normal matrix and right-hand-side vector for a given solution parameter set.
SOLVE	Solves normal equations to obtain corrections to solution parameter estimates.

The mathematical formulation for POWSER is given in Ref. 10. The principal reference for NORM is Ref. 11. SOLVE is documented in Ref. 12. Auxiliary programs are available for performing operations on the normal matrix and right-hand-side vector before entering SOLVE. APRIOR is used for adding a priori constraints and VMERGE is used for combining sets of normal equations obtained from different sources. In particular, a combined solution may be obtained using different sets of measurements (e.g. range and Doppler) taken for the same data arc.

II. Extended Capability for Entry Reconstruction

A new program element has been developed for computing the normal equations for the accelerometer "data type". It has been assigned the acronym PVETNA (Pioneer Venus Entry Trajectory Normal Equations for Accelerometry), and has been designed to operate in consonance with the existing program elements (POWSER , SOLVE). In effect, it is the counterpart of NORM for accelerometer measurements. The solution parameters currently provided are: S/C initial conditions; ballistic coefficient C_D' ($C_DA/2W$); angle-of-attack (α); side-slip angle (β); and accelerometer biases. Single or multi-axis accelerometer measurements may be processed. For multi-axis measurements, each axis is treated as a separate "data type" and the output normal matrix/right-hand-side vector is for the combined normal equations. The 3-D POST program (Ref. 13) was used for verification of the observation models.

The interaction of all program elements, with the appropriate file interfaces, is shown in Fig. B-1.

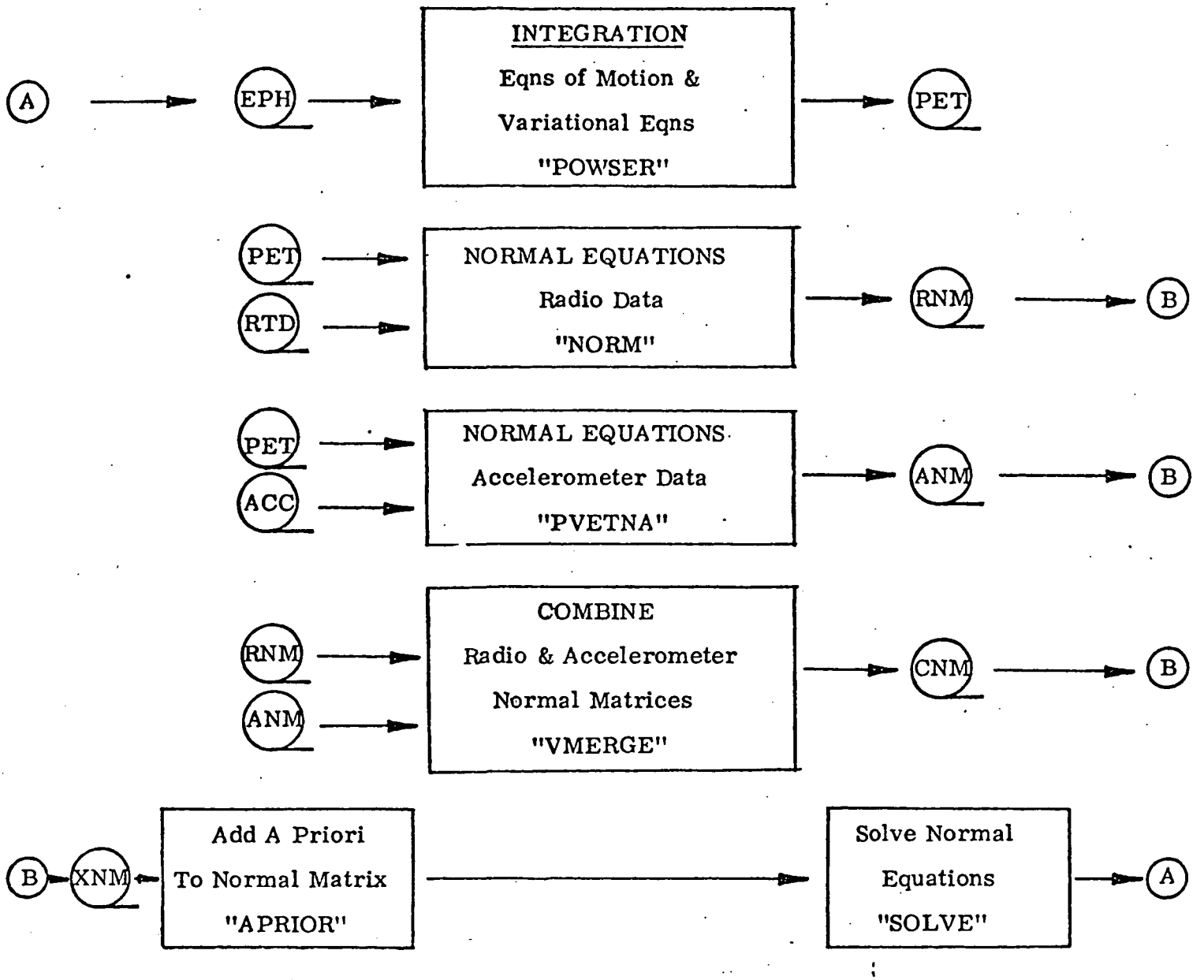

EPH: JPL Planetary Ephemeris
PET: Probe (S/C) Ephemeris Tape
RTD: Radio Tracking Data (Doppler)
ACC: Accelerometer Measurements

RNM: Radio Normal Matrix
ANM: Accelerometer Normal Matrix
CNM: Combined Normal Matrix (Radio & Accelerometer)
XNM: Any of the Matrices-- RNM, ANM, CNM

Fig. B-1 PIONEER VENUS ENTRY SCIENCE SOFTWARE

(FUNCTIONAL FLOW DIAGRAM)

APPENDIX C

MEASUREMENT SENSITIVITIES TO SOLUTION PARAMETERS

For the nominal entry conditions given in Sec. III, the first order sensitivities of the accelerometer and Doppler (range rate) data types to the solution parameters were plotted for the upper entry region (E to E+40^s). The sensitivities are significant in that they describe the residual "signature" associated with each parameter. The sensitivities are always trajectory-dependent, however, and care must be taken not to extrapolate results to other trajectories. One other very important point is that being "first order" sensitivities, they may only be used to predict the effect of small errors.

Accelerometer sensitivity curves are presented in Figs. C-1 through C-5. The units for each partial derivative, shown in the upper right corner of each frame, are m/sec^2 per model parameter unit. (e.g. $\partial A_x/\partial V$ = m/sec^2 per km/sec). Fig. C-1 shows the accelerometer sensitivity with respect to V, γ; C-2 for ψ, Radius (altitude); C-3 for φ, λ (right ascension); C-4 for $C_D' = (C_D A/2W)$. Fig. C-5 shows the sensitivity with respect to angles of attack (α) and side-slip (β). Since the nominal accelerometer data were generated assuming α, $\beta = 0$, the sensitivity with respect to each of these parameters is identically zero, because the measured acceleration is a cosine projection of both angles and its sensitivity is a sine projection. Therefore, Fig. C-5 was generated using $\alpha = 5^o$, $\beta = 5^o$. The α, β sensitivities are identical, again because of the cosine projection of each angle.

In general, Figs. C-1 through C-5 show pronounced sensitivity of the accelerometer data type to V, γ, h, C_D', α, β and virtually no sensitivity to ψ, φ, λ as expected. In all cases, the sensitivities are near-zero both prior to and after the peak g period. Therefore, the information content, if any, is contained in an interval of about 4 seconds around peak g, which occurs at about 11 sec. The C_D' sensitivity plot (Fig. C-4) requires some clarification. The sensitivity is for a unit change in a parameter whose nominal value is $\sim 3 \times 10^{-9}$. C_D', as used in this report, represents a density scale factor. Since the nominal value for a density scale factor is 1, the C_D' sensitivity curve should

be adjusted by the nominal value of C_D' (i.e. multiplied by 3×10^{-9}). Therefore, a 10% density scale factor error should have a maximum effect of about 90 m/sec^2 [$(3 \times 10^{-9}) \times (3 \times 10^{11}) \times 0.1$] on accelerometer measurements.

Range rate sensitivity curves are shown in Figs. C-6 through C-9. The units for each partial derivative, shown in the upper right corner of each frame, are m/sec per model parameter unit. (e.g. $\partial \dot{r} / \partial V$ = m/sec per km/sec). Fig. C-6 shows range rate sensitivity with respect to V, γ; C-7 for ψ, Radius (altitude); C-8 for φ, λ (right ascension); C-9 for $C_D' = (C_D A/2W)$. For the drag-only model assumed, the S/C trajectory (and hence the range rate data) is independent of angle of attack (α) and side-slip (β). Therefore, range rate sensitivities to these parameters do not exist.

In contrast to the accelerometer sensitivities, range rate is sensitive to all model parameters, as shown in Figs. C-6 through C-9. Range rate data after the peak g period is very insensitive to model parameter errors, as was accelerometry. Unlike accelerometry, however, range rate data prior to peak g has pronounced sensitivity to errors in V, γ and modest sensitivity to ψ, φ, λ. Along with accelerometry range rate data is quite insensitive to small altitude errors both prior to and after peak g. Range rate sensitivity curves for ψ, φ, λ are very similar in appearance and indicate fairly strong coupling among these parameters. In considering the range rate sensitivity with respect to a density scale factor error rather than a C_D' error, one should adjust the C_D' curve via a multiplication factor of 3×10^{-9}. Therefore, a 10% density scale factor error should have a maximum effect of about 21 m/sec [$(3 \times 10^{-9}) \times (7 \times 10^{11}) \times 0.1$] on range rate measurements.

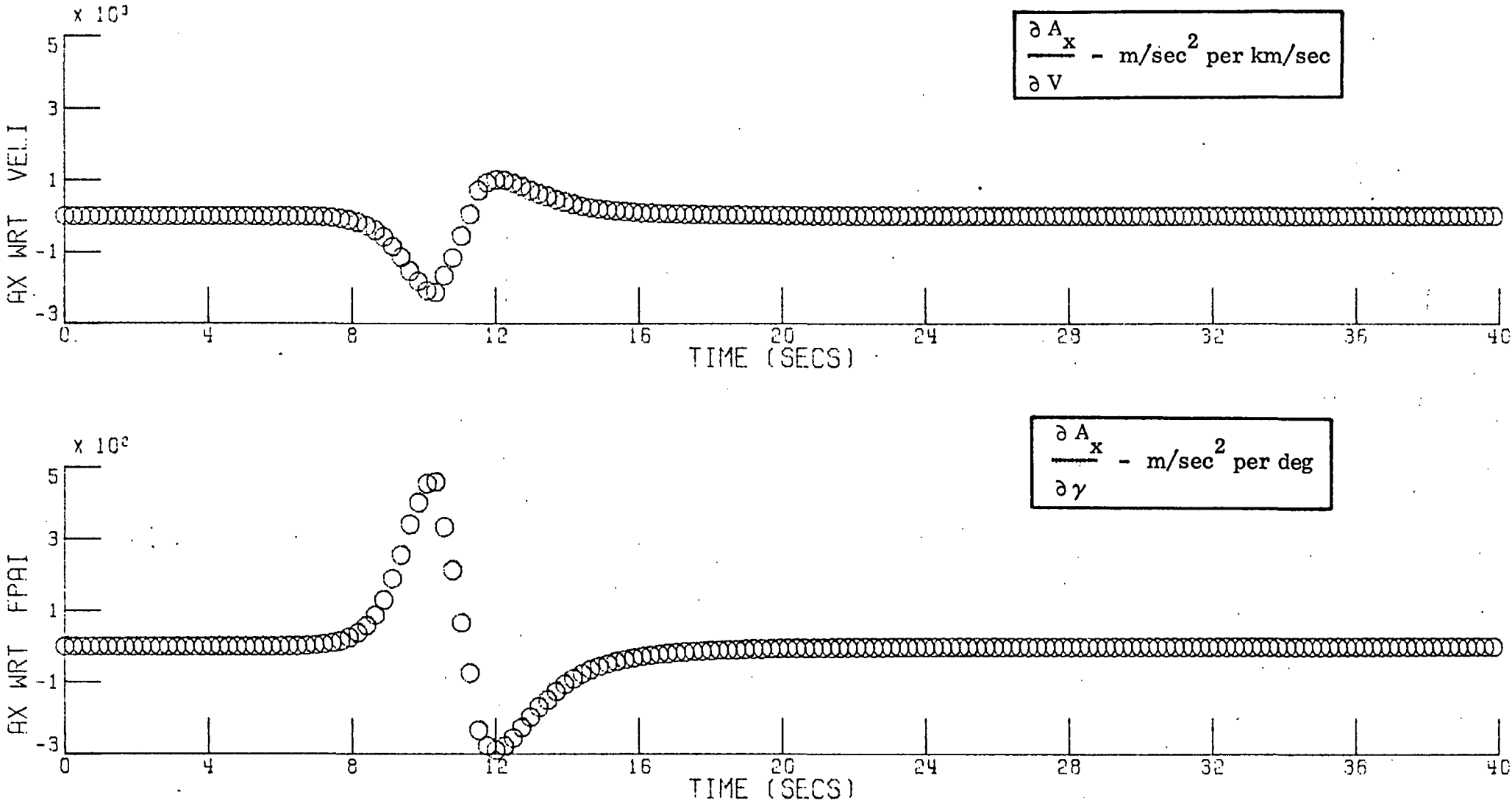

Fig. C-1 ACCELEROMETER SENSITIVITY PLOTS (V, γ) VS TIME FROM ENTRY

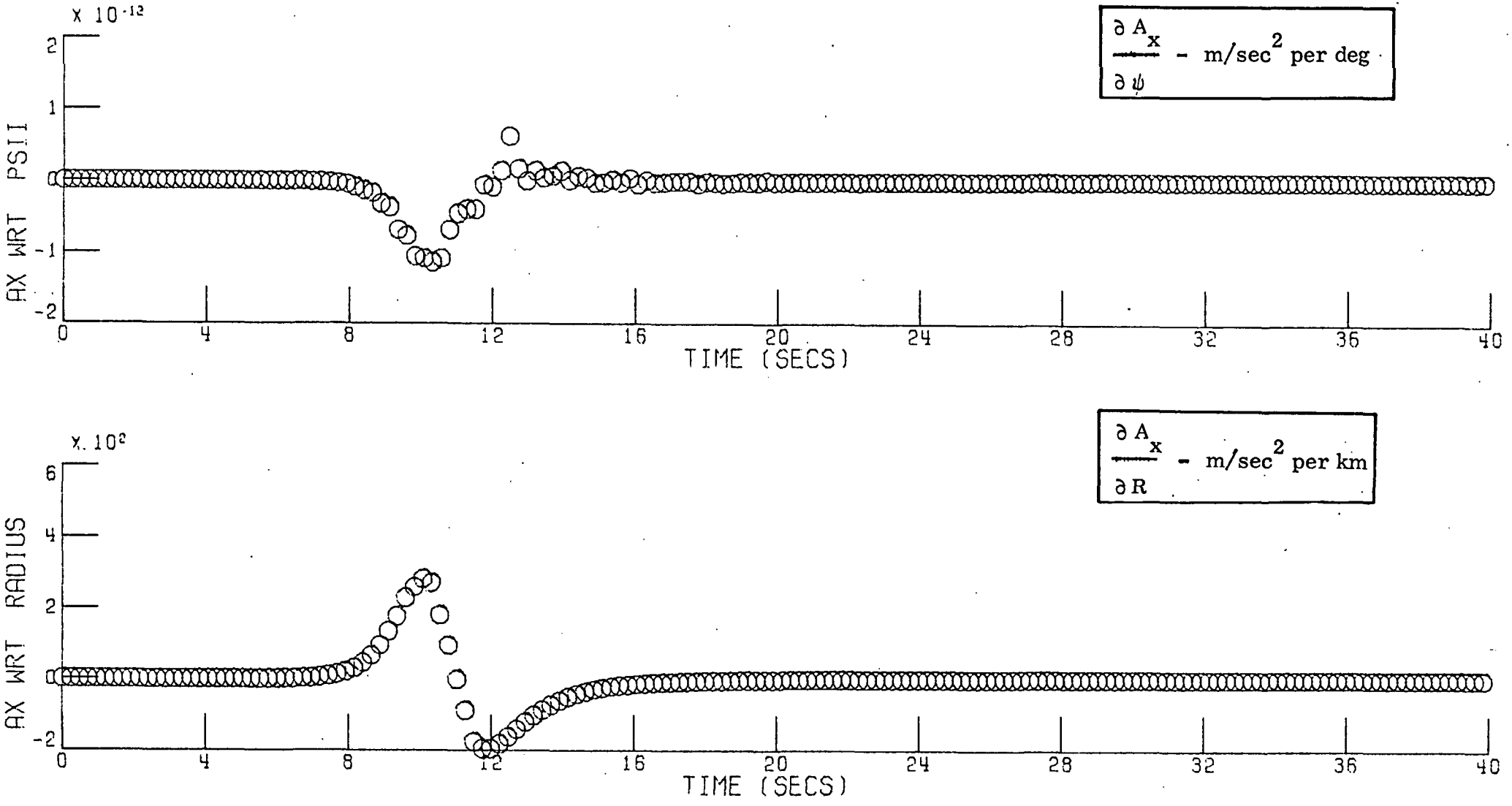

Fig. C-2 ACCELEROMETER SENSITIVITY PLOTS (ψ , R) VS TIME FROM ENTRY

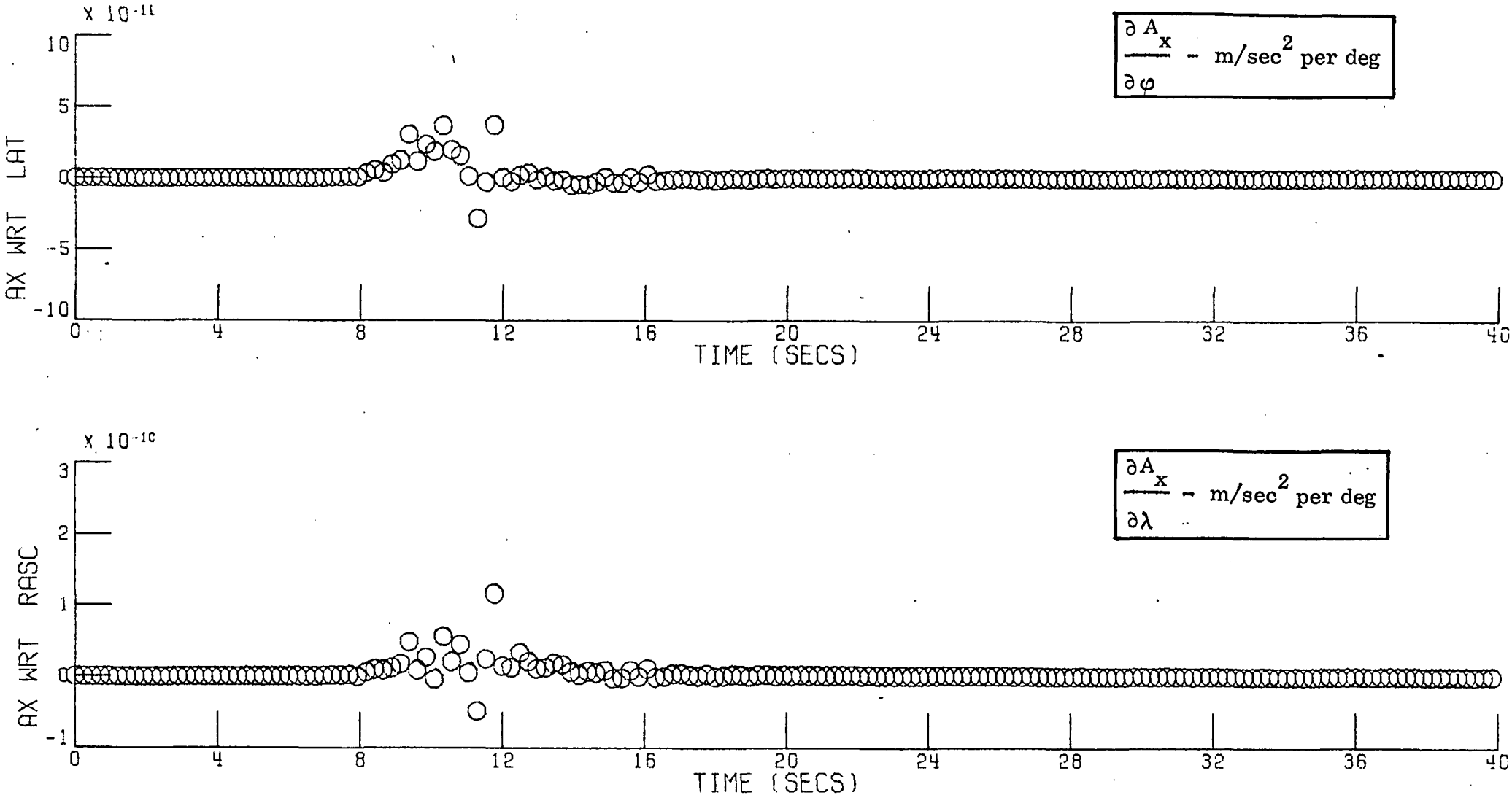

Fig. C-3 ACCELEROMETER SENSITIVITY PLOTS (φ , λ) VS TIME FROM ENTRY

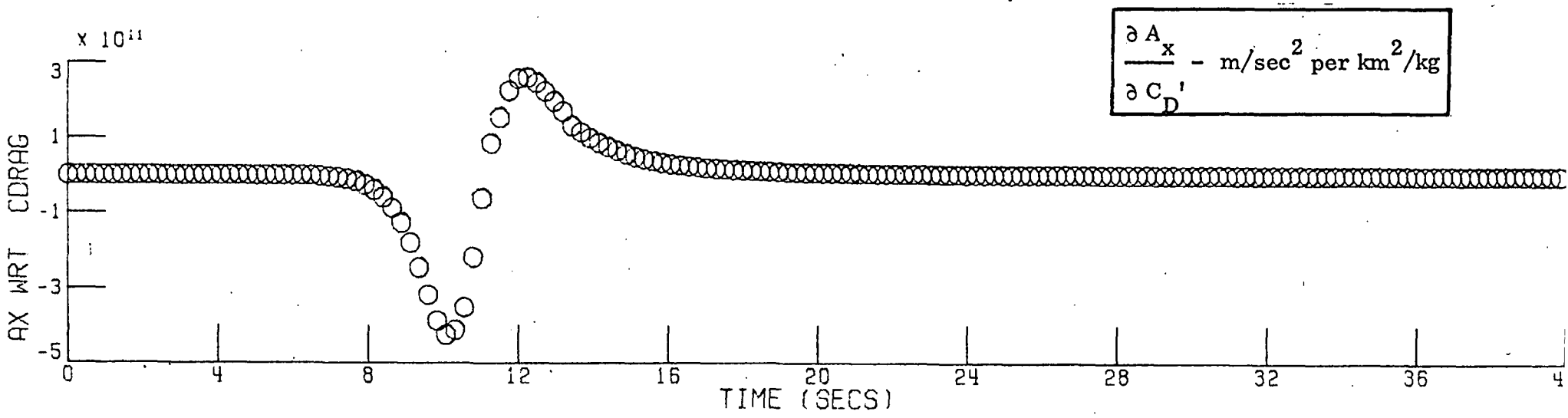

Fig. C-4 ACCELEROMETER SENSITIVITY TO C_D' VS TIME FROM ENTRY

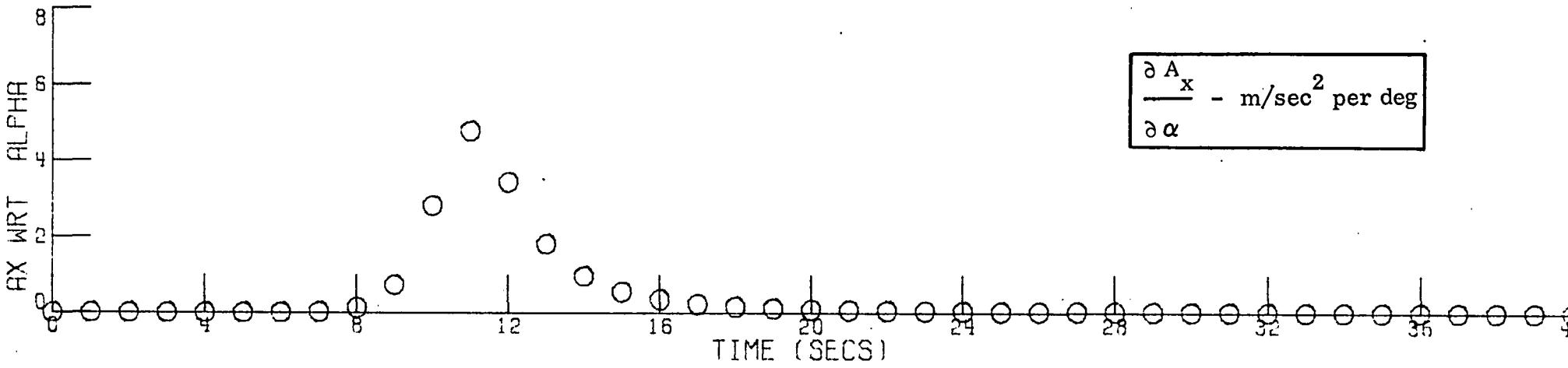

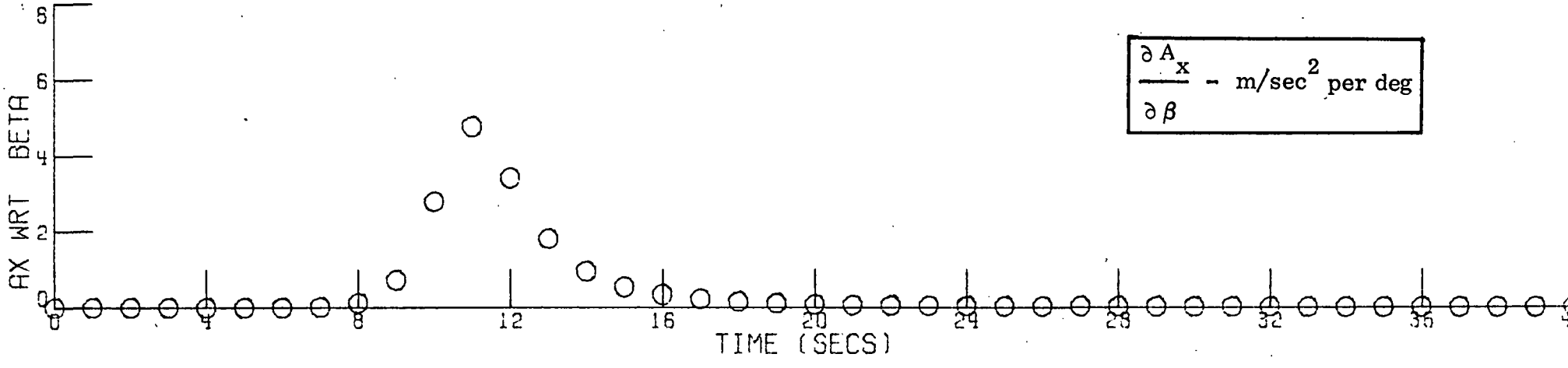

Fig. C-5 ACCELEROMETER SENSITIVITY PLOTS (α , β) VS TIME FROM ENTRY

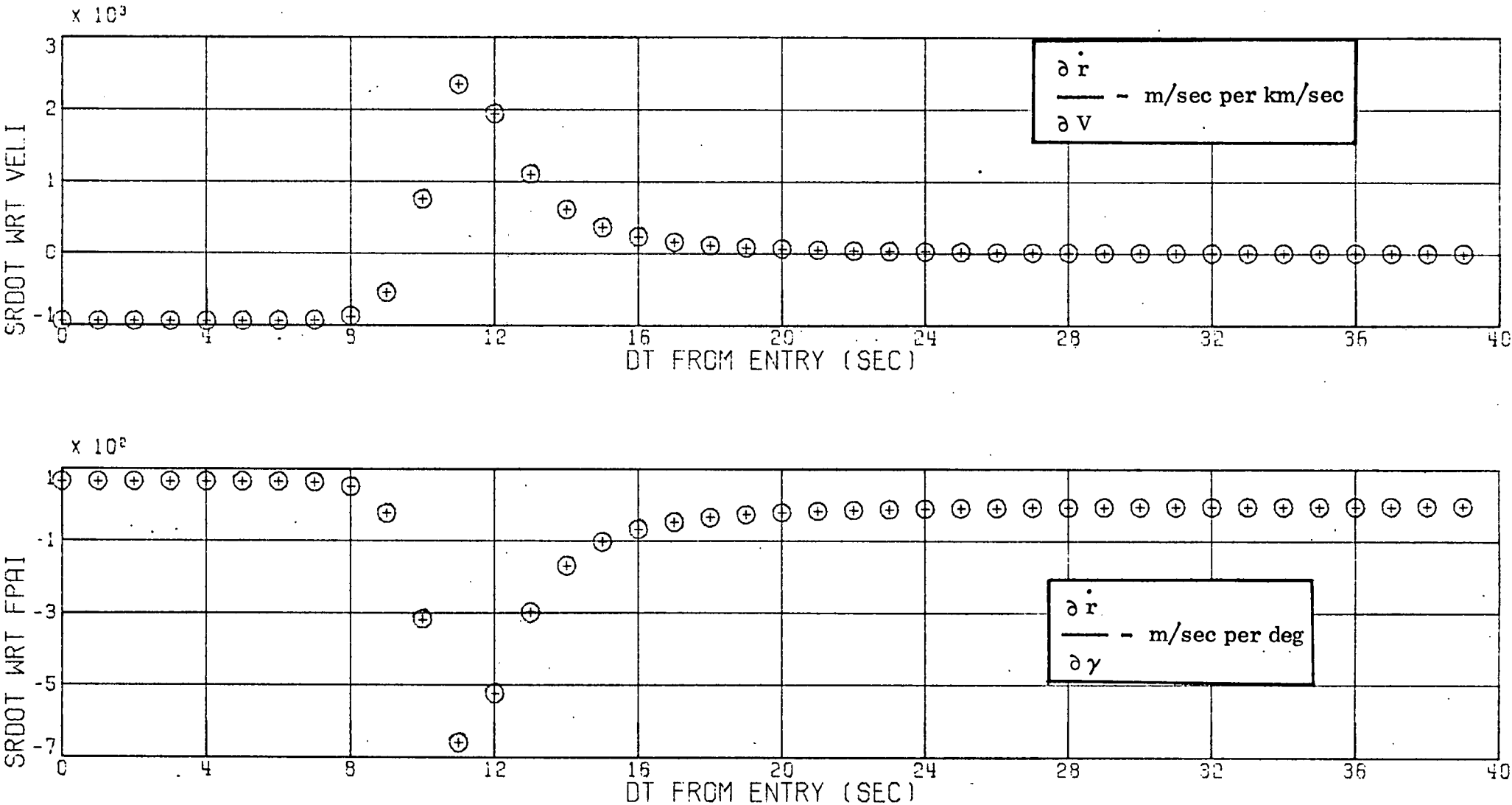

Fig. C-6 RANGE RATE SENSITIVITY PLOTS (V , γ) VS TIME FROM ENTRY

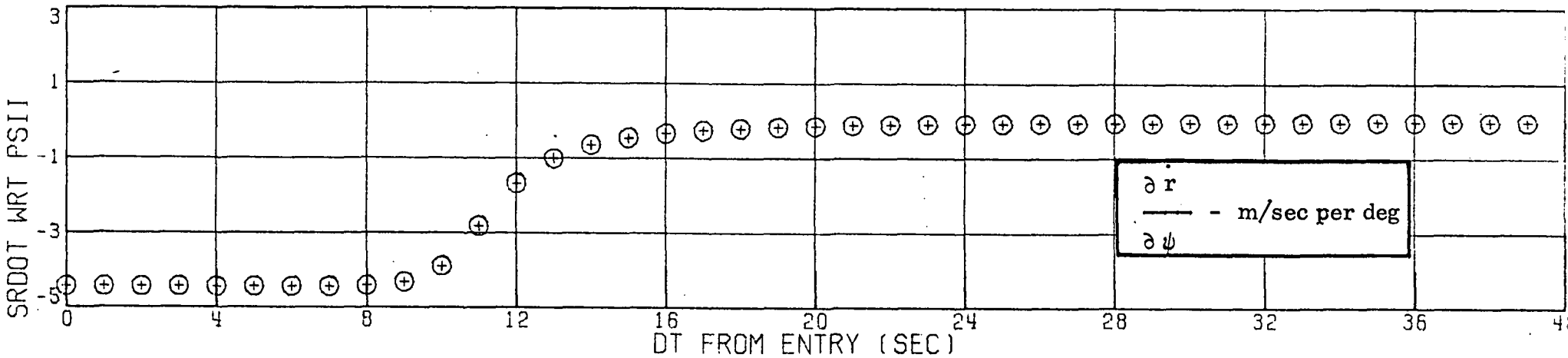

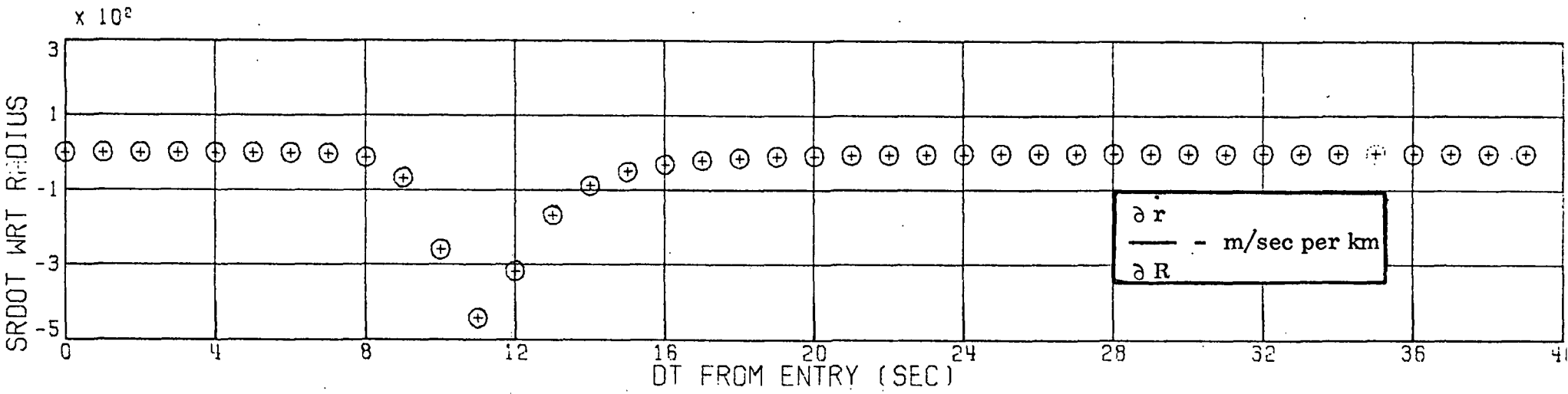

Fig. C-7 RANGE RATE SENSITIVITY PLOTS (ψ , R) VS TIME FROM ENTRY

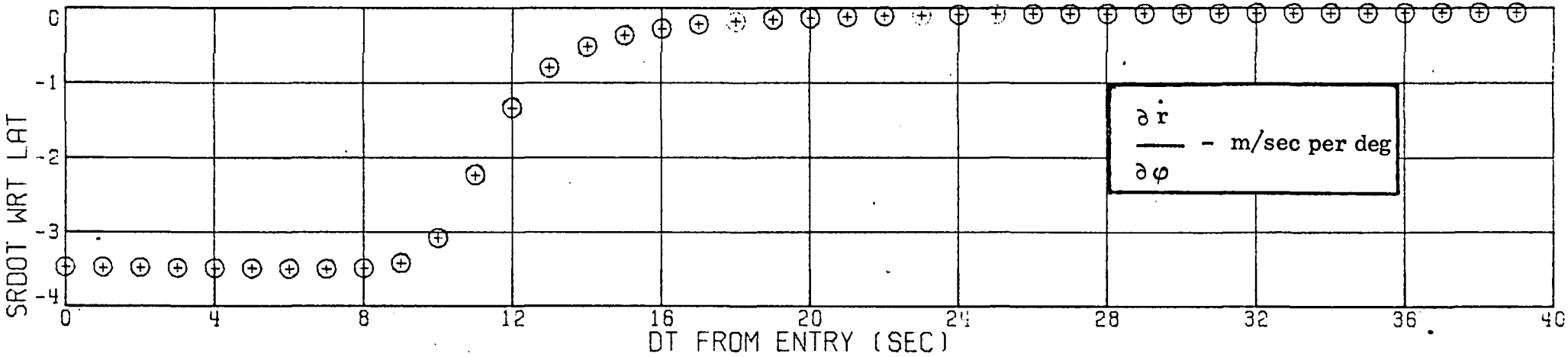

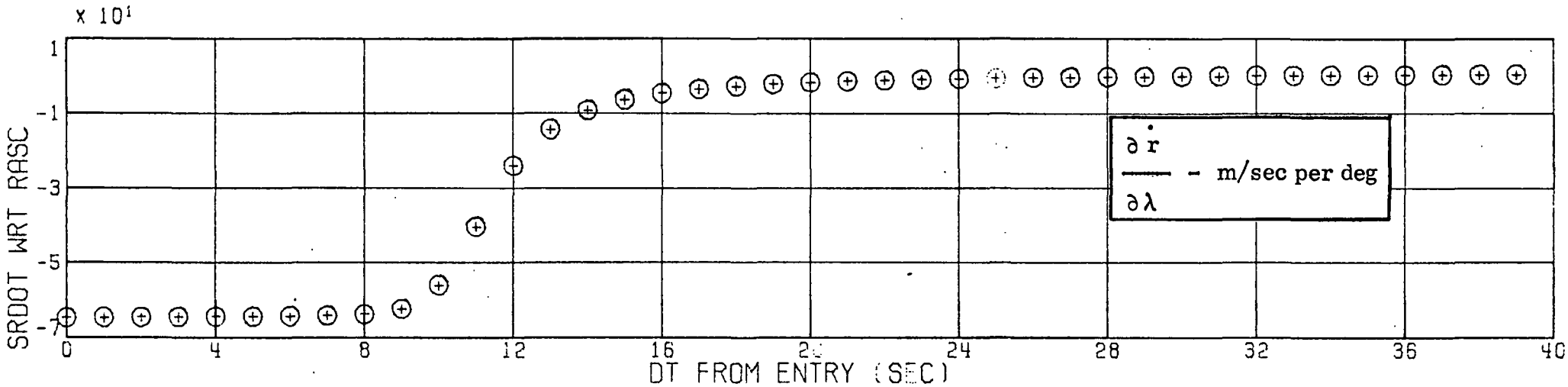

Fig. C-8 RANGE RATE SENSITIVITY PLOTS (φ , λ) VS TIME FROM ENTRY

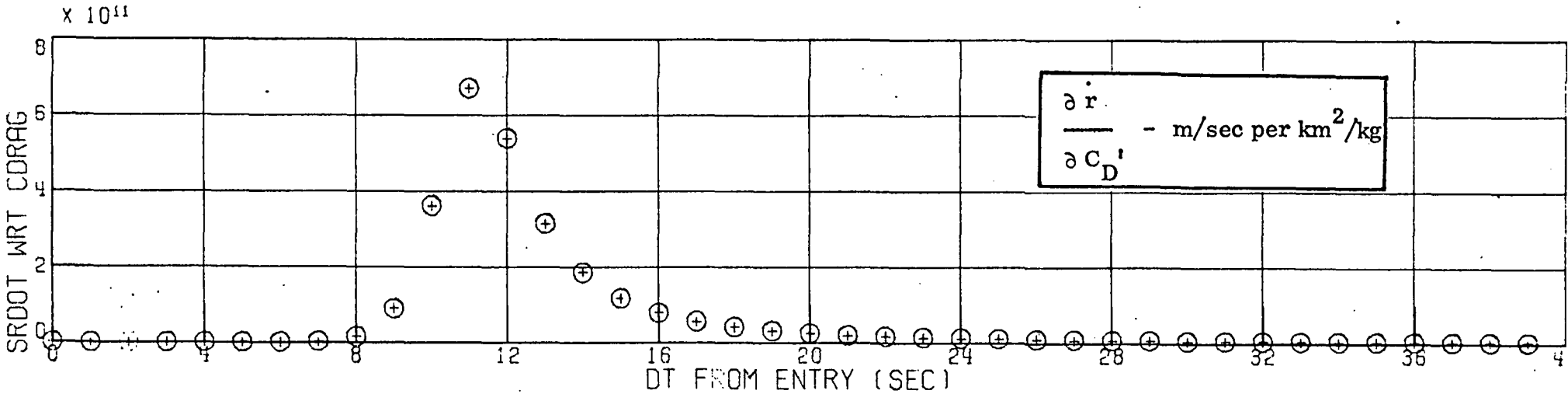

Fig. C-9 RANGE RATE SENSITIVITY TO C_D' VS TIME FROM ENTRY

APPENDIX D

EFFECT OF VARIOUS DENSITY MODELS ON CONVENTIONAL PREDICTION

The batch orbit determination method evaluated in this report for applicability to reconstruct the multi-probe entries uses conventional Cowell integration to obtain spacecraft state prediction. As a consequence it is dependent upon a priori modelling of the spacecraft and atmospheric parameters. Reference 3 gives six (6) possible Venus atmosphere models. These models are defined as follows:

Model No.	Description
I	Most Probable Molecular Mass and Mean Solar Activity
II	Maximum Molecular Mass and Minimum Solar Activity
III	Maximum Molecular Mass and Maximum Solar Activity
IV	Minimum Molecular Mass and Minimum Solar Activity
V	Minimum Molecular Mass and Maximum Solar Activity
VI	Maximum Molecular Mass and Night-Side Exospheric Temperature

These models were based on the occultation results of both Mariner 2 and 5 as well as the entry measurements made by the USSR Venera Spacecraft 4 - 7, inclusive. Model I was adopted as the reference atmosphere for the entry analysis conducted in this report.

It is instructive to show the effect of the various atmospheres on the multi-probe trajectory. Figures D-1 and D-2 show trajectory differences in V, γ, h and axial acceleration incurred due to the various models. The reference trajectory compared against is that obtained for Model I. Only two figures need be shown since there are only three distinct atmospheres in the altitude range (h_o=150 km) covered during the first 300 seconds of entry flight. Models II, III and VI (maximum molecular mass models) all induce the same dispersions relative to Model I. Models IV and V, the minimum molecular mass models, produce almost identical deviations relative to the reference model.

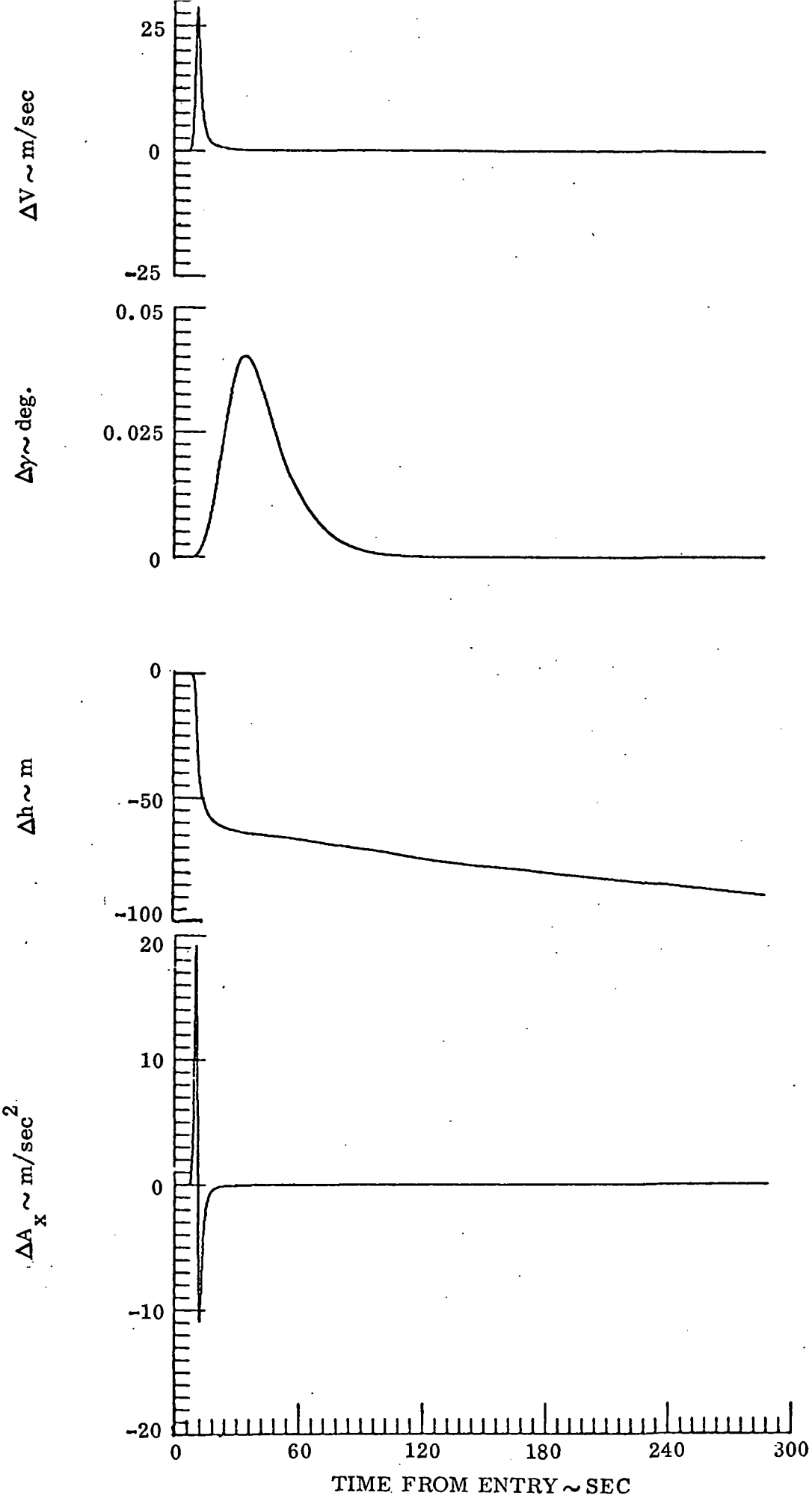

Fig. D-1 TRAJECTORY DIFFERENCES - MAXIMUM MOLECULAR MASS MODEL VS. MODEL I

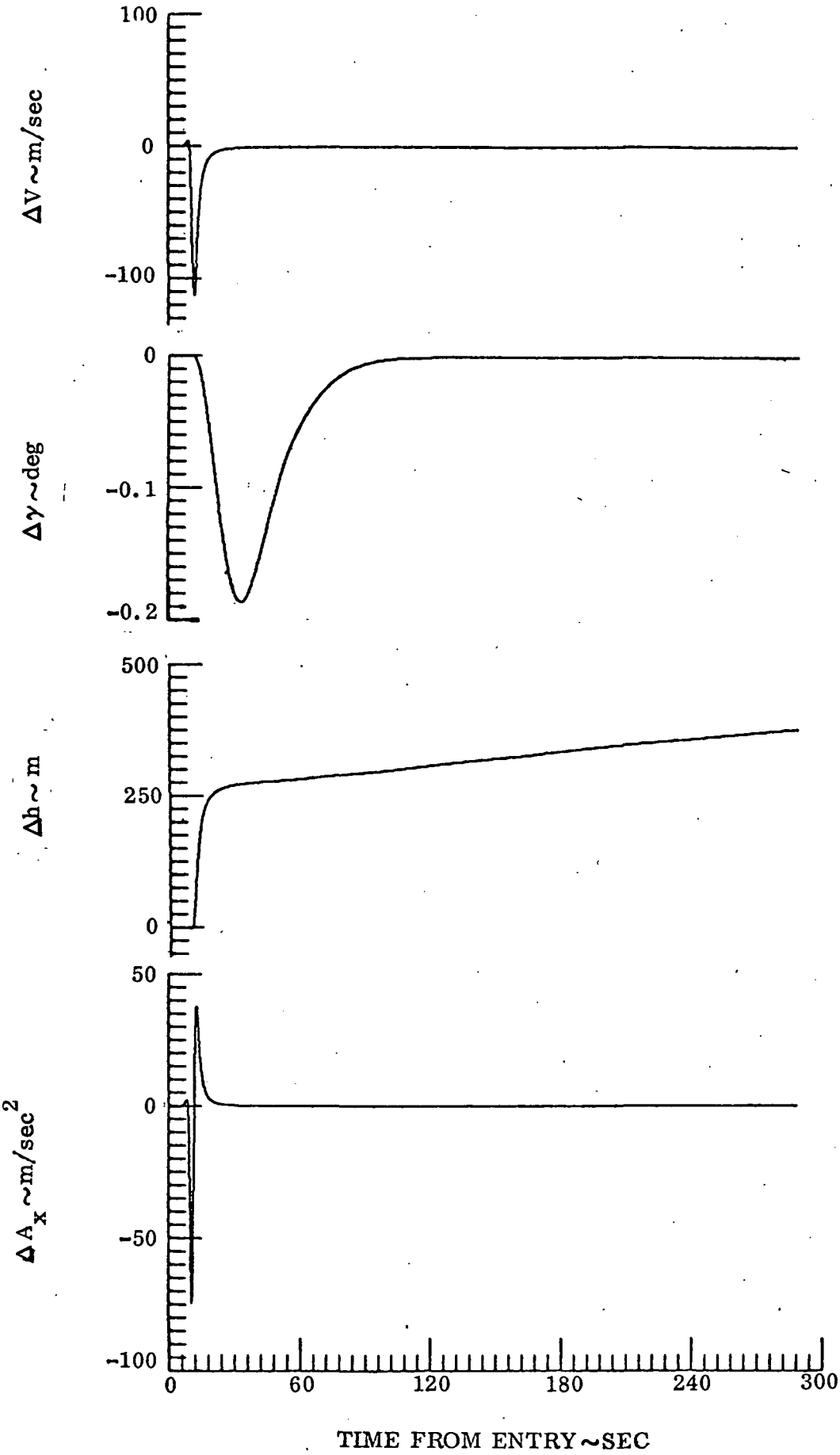

Fig. D-2 TRAJECTORY DIFFERENCES - MINIMUM MOLECULAR MASS MODEL VS. MODEL I

APPENDIX E

THE IMPORTANCE OF PROBE ATTITUDE KNOWLEDGE

In Section IV. C. 1 the importance of knowledge of the spacecraft attitude was discussed. It was stated therein that both the deterministic and conventional batch methods were dependent upon some presumed estimate. The deterministic scheme needs some reasonable estimate of the alignment of the body mounted accelerometry with respect to the relative velocity vector to do deterministic prediction. The conventional method, which processes the accelerometer measurements as observables, needs to know this same orientation to properly compute the accelerations, i.e., to account for any misalignment between the spacecraft x-axis and the drag force. This attitude information is not important for prediction in the conventional method since the "drag-only" probe trajectories are essentially unaffected. (1)

The best information available to prescribe S/C attitude, at least as a priori data, must necessarily come from a full six-degree-of-freedom simulation. These data could be generated as soon as the best estimates of the actual probe entry conditions are available from the JPL. Preliminary results have been obtained from ARC. Much insight as to the importance of the S/C attitude knowledge can be gained from these preliminary data. Fig. E-1 shows the attitude time history for a typical probe, spinning at approximately 15 RPM. Insufficient data were available to completely describe the dynamics. Plotted are the angle-of-attack (α) and side-slip angle (β) versus time. Also shown is the total angle-of-attack (η). This angle represents an envelope describing the total excursion between the x-axis accelerometer and the drag direction due to the spinning dynamics. Actually the spacecraft is spiralling inward to a trim condition. An approximate 2^{o} steady-state η is achieved after 12 seconds.

Max g , and various lesser g levels are superimposed on the time scale in the figure. Certainly the large attitude excursions early on are insignificant since the S/C has not penetrated sensible atmosphere. However, the non-trivial

(1) The drag is only affected by $\sim 10\%$ over a 30^{o} range of angle-of-attack, $< 2\%$ over a 10^{o} variation (see Fig. III-2 of the report). Moreover, the maximum lift coefficient throughout the entire 30^{o} variation is only -0.016, i.e., the L/D is everywhere < 0.015.

attitude excursions which occur during peak g are significant for the small probes. Indeed they represent sensed loss of ΔV since there is only a single axis accelerometer. In fact, the sensed loss is ~10 mps for the attitude history shown. This can be equivalenced to an approximate 3.4^{o} residual attitude error or a 0.17% scale factor error. Again, the actual ΔV undergone at the spacecraft is essentially unaffected.

Clearly, this attitude must be accounted for to obtain reasonable deterministic prediction. If not accounted for in the conventional scheme when processing the accelerometry the error in the computed observable will be on the order of 0.5 g's. This may not be significant, specifically when processing the ΔV derived accelerometry since this error is well within the expected noise during BLACKOUT II. However, it will everywhere appear as a bias in the computed observable, i.e., the actual observable will be less than the computed observable if the latter is based on an assumed zero angular deviation (or the actual angular deviation is greater than that assumed).

There are some problems associated with using a pre-flight attitude time history for spacecraft attitude. First, the actual time of peak g may vary by a second or so from the best a priori estimate. Seemingly, this could be biased out since the spiralling dynamics are physically tied to the acceleration as it increases. A second problem which can occur is the simple fact that the actual trim condition reached may not equal the pre-flight estimate. If it is, within less than 1^{o}, these would be no problem in disregarding this in the conventional method. If needed, an equivalent scale factor or attitude bias could be solved for as suggested in the Report.

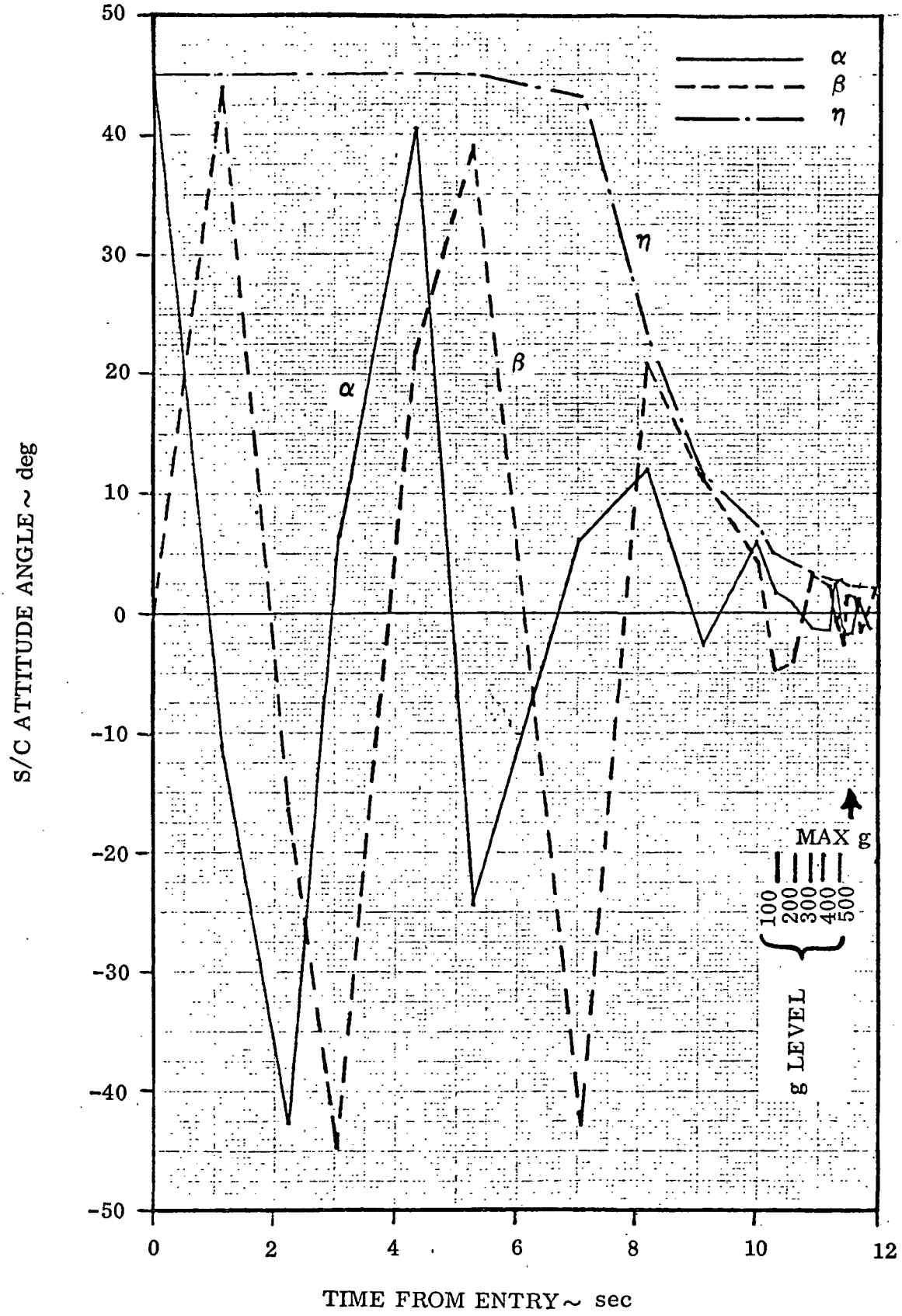

Fig. E-1 TYPICAL P/V PROBE ATTITUDE TIME HISTORY

REFERENCES

(1) "Formulation on Statistical Trajectory Estimation Programs"; W. E. Wagner and A. C. Serold; NASA CR-1482; January, 1970.

(2) "Linear Filtering of Ballistic-Entry Probe Data for Atmospheric Reconstruction"; M. L. Sabin; Journal of Spacecraft and Rockets, Vol. 12, No. 2; September 1974.

(3) "Constants and Related Information for Astrodynamics Calculations, 1968"; W. G. Melbourne, et. al; JPL TR 32-1306; July 15, 1968.

(4) "Models of Venus Atmosphere (1972)"; NASA SP-8011; NASA Space Vehicle Design Criteria Monograph (Environment); principal authors R. B. Noll (Aerospace Systems, Inc.) and Dr. M. B. McElroy (Harvard University); prepared under cognizance of NASA GSFC; revised September, 1972.

(5) "Polynomial Expressions for Planetary Equators and Orbit Elements With Respect to the Mean 1950.0 Coordinate System"; F. M. Sturms, Jr; JPL TR 32-1508; January 15, 1971.

(6) "JPL Development Ephemeris Number 96"; E. M. Standish, Jr., et. al; JPL TR 32-1603; February 29, 1976.

(7) "Accuracy Assessment of First Order In Situ Pioneer/Venus Density Estimation Using a Single Altitude Fix"; J. T. Findlay; AMA Report No. 78-13; May, 1978.

(8) "Atmospheric Density Reconstruction Accuracies Using a Wind Estimator During the Viking Aeroshell Entry"; J. T. Findlay; AMA Report No. 72-51; November, 1972.

(9) "Spline Functions, Interpolation, and Numerical Quadrature"; T. N. E. Greville; in Mathematical Methods for Digital Computers - Vol. II (2nd Edition); Edited by Drs. A. Ralston and H. Wilf; J. Wiley and Sons, Inc.

(10) "Mathematical and Programming Documentation of a General Purpose Integrator Using Power Series Methods"; J. G. Hartwell and T. R. Lewis; DBA Systems, Inc; Contract NAS1-9389; December, 1969.

(11) "Mathematical Formulation of the Double-Precision Orbit Determination Program (DPODP)"; T. D. Moyer; JPL TR 32-1527; May 15, 1971.

(12) "Lunar Gravitational Field in Spherical Harmonics (LUNGFISH)", Book 1 - Mathematical Description; CUC, Inc.; prepared under NAS1-4998; Feb. 1966.

(13) "Program to Optimize Simulated Trajectories (POST)"; Vols. I thru III; G. L. Brauer, et al; NASA CR-132689; April, 1975.